




RESEARCH

Open Access



# Assessment of the toxicity and carcinogenicity of double-walled carbon nanotubes in the rat lung after intratracheal instillation: a two-year study

Dina Mourad Saleh<sup>1,2,3</sup> , Shengyong Luo<sup>4</sup>, Omnia Hosny Mohamed Ahmed<sup>1,2,5</sup>, David B. Alexander<sup>1\*</sup> , William T. Alexander<sup>1</sup>, Sivagami Gunasekaran<sup>1,2</sup>, Ahmed M. El-Gazzar<sup>6</sup>, Mohamed Abdelgied<sup>7,8</sup>, Takamasa Numano<sup>1</sup>, Hiroshi Takase<sup>9</sup>, Makoto Ohnishi<sup>10</sup>, Susumu Tomono<sup>11</sup>, Randa Hussein Abd el Hady<sup>3</sup>, Katsumi Fukamachi<sup>12</sup>, Jun Kanno<sup>13</sup>, Akihiko Hirose<sup>13</sup>, Jiegou Xu<sup>1,14</sup>, Shugo Suzuki<sup>15</sup>, Aya Naiki-Ito<sup>2</sup>, Satoru Takahashi<sup>2</sup> and Hiroyuki Tsuda<sup>1\*</sup> 

## Abstract

**Background:** Considering the expanding industrial applications of carbon nanotubes (CNTs), safety assessment of these materials is far less than needed. Very few long-term in vivo studies have been carried out. This is the first 2-year in vivo study to assess the effects of double walled carbon nanotubes (DWCNTs) in the lung and pleura of rats after pulmonary exposure.

**Methods:** Rats were divided into six groups: untreated, Vehicle, 3 DWCNT groups (0.12 mg/rat, 0.25 mg/rat and 0.5 mg/rat), and MWCNT-7 (0.5 mg/rat). The test materials were administered by intratracheal-intrapulmonary spraying (TIPS) every other day for 15 days. Rats were observed without further treatment until sacrifice.

**Results:** DWCNT were biopersistent in the rat lung and induced marked pulmonary inflammation with a significant increase in macrophage count and levels of the chemotactic cytokines CCL2 and CCL3. In addition, the 0.5 mg DWCNT treated rats had significantly higher pulmonary collagen deposition compared to the vehicle controls. The development of carcinomas in the lungs of rats treated with 0.5 mg DWCNT (4/24) was not quite statistically higher ( $p = 0.0502$ ) than the vehicle control group (0/25), however, the overall incidence of lung tumor development, bronchiolo-alveolar adenoma and bronchiolo-alveolar carcinoma combined, in the lungs of rats treated with 0.5 mg DWCNT (7/24) was statistically higher ( $p < 0.05$ ) than the vehicle control group (1/25). Notably, two of the rats treated with DWCNT, one in the 0.25 mg group and one in the 0.5 mg group, developed pleural mesotheliomas. However, both of these lesions developed in the visceral pleura, and unlike the rats administered MWCNT-7, rats administered DWCNT did not have elevated levels of HMGB1 in their pleural lavage fluids. This indicates that the mechanism by which the mesotheliomas that developed in the DWCNT treated rats is not relevant to humans.

\*Correspondence: dalexand@phar.nagoya-cu.ac.jp; htsuda@phar.nagoya-cu.ac.jp

<sup>1</sup> Nanotoxicology Lab Project, Nagoya City University, 3-1 Tanabe-Dohri, Mizuho-ku, Nagoya 467-8603, Japan  
Full list of author information is available at the end of the article



© The Author(s) 2022. **Open Access** This article is licensed under a Creative Commons Attribution 4.0 International License, which permits use, sharing, adaptation, distribution and reproduction in any medium or format, as long as you give appropriate credit to the original author(s) and the source, provide a link to the Creative Commons licence, and indicate if changes were made. The images or other third party material in this article are included in the article's Creative Commons licence, unless indicated otherwise in a credit line to the material. If material is not included in the article's Creative Commons licence and your intended use is not permitted by statutory regulation or exceeds the permitted use, you will need to obtain permission directly from the copyright holder. To view a copy of this licence, visit <http://creativecommons.org/licenses/by/4.0/>. The Creative Commons Public Domain Dedication waiver (<http://creativecommons.org/publicdomain/zero/1.0/>) applies to the data made available in this article, unless otherwise stated in a credit line to the data.

**Conclusions:** Our results demonstrate that the DWCNT fibers we tested are biopersistent in the rat lung and induce chronic inflammation. Rats treated with 0.5 mg DWCNT developed pleural fibrosis and lung tumors. These findings demonstrate that the possibility that at least some types of DWCNTs are fibrogenic and tumorigenic cannot be ignored.

**Keywords:** Double walled carbon nanotubes, Two-year study, Toxicity, Carcinogenicity, Rats

## Background

Carbon nanotubes (CNTs) are composed of concentric one-atom thick graphene cylinders and have a wide range of applications [1]. The ability to manipulate the lengths and the number of graphene cylinders that compose CNTs has allowed the production of specific CNTs with different lengths and thicknesses, and these differences result in different CNTs having different physical properties. In general, CNTs are divided into two types single-walled carbon nanotubes (SWCNT) and multi-walled carbon nanotubes (MWCNTs) with double-walled carbon nanotubes (DWCNT) sometimes being considered a distinct class of MWCNT. Multi-walled carbon nanotubes can be divided into two general subtypes, tangled and straight.

The very light weight of CNTs make them easily airborne and inhaled. Consequently, the possibility that CNTs may exhibit foreign body toxicity in the airways and pleura is of concern [2–7]; also see Hansen and Lennquist 2020 [8]. Harmful fibrous particles like asbestos are known to induce fibrosis and cancer through chronic unresolved inflammation characterized by inflammatory cell accumulation and production of reactive oxygen and nitrogen species (ROS & RNS) that can damage DNA and through repeated cycles of tissue damage and repair fix potentially transforming mutations into daughter cells [9–15].

Despite the widespread production and use of CNTs very few *in vivo* studies with a duration of 18 months or more have been carried out to assess the toxicity and carcinogenicity of these materials in experimental animals [16–24]. At the time of this writing, IARC has evaluated only MWCNT-7 as carcinogenic in experimental animals and as being possibly carcinogenic in humans (Group 2B). All other CNTs had inadequate evidence in experimental animals for carcinogenicity and they were not classifiable as to their carcinogenicity to humans [11].

We have established that instillation of insoluble test materials, such as CNTs, into the rat lung every other day over the course of 2 weeks (8 doses in total) results in distribution of the test material throughout each of the lung lobes [25]; we refer to this instillation procedure as intratracheal intrapulmonary instillation (TIPS). Using TIPS, we assessed the toxicity and carcinogenicity of MWCNT-N, MWCNT-7, MWCNT-A,

and MWCNT-B in long term studies. The thick straight MWCNT-N (40 layers) induced both lung tumors and malignant pleural mesotheliomas [23]; MWCNT-7 (more than 40 layers) induced malignant pleural mesotheliomas [20]; a thin tangled MWCNT, referred to as MWCNT-B, (15 layers) induced lung tumors [22] and MWCNT-A (very thick 150 layers) was shown to be a likely lung carcinogen [22].

However, very little is known about the *in vivo* toxic effect of DWCNTs. The only available results are short term studies in mice and our short term study in rats. Crouzier et al. found inflammatory reactions in mice 6, 24, and 48 h after a single intranasal instillation of 1.5 mg/kg DWCNT (1.2–3.5 nm diameter, 1–10  $\mu\text{m}$  length) [26]. Tian et al. found that in mice inflammatory lesions were not resolved after a 7 day observation period after a single intratracheal instillation of 50  $\mu\text{g}$  DWCNT (3.5 nm diameter, 1–10  $\mu\text{m}$  length) [27]. Sager et al. reported that mice administered 40  $\mu\text{g}$  DWCNT (1–2 nm diameter, <5  $\mu\text{m}$  length) by pharyngeal aspiration had developed alveolitis and lung fibrosis 56 days after administration of the DWCNT [28]. O’Shaughnessy et al. exposed mice to DWCNT by whole body inhalation at a dose of 10.8 mg/m<sup>3</sup>, 4 h/day for 5 days. DWCNT caused inflammation and tissue injury to the lung which was resolved 2 weeks after the end of exposure [29]. El-Gazzer et al. administered DWCNT (1–3 nm diameter, due to the tangled nature of the fibers the length could not be measured) and MWCNT-7 (55.5  $\pm$  12 nm diameter, 6.5  $\pm$  2.4  $\mu\text{m}$  length) by TIPS to rats. Six weeks after administration the degree of pulmonary and pleural toxicity induced by MWCNT-7 was much higher than that induced by DWCNT. DWCNT caused more extensive granulation tissue formation encapsulating the fibers than MWCNT-7 [30]. In mice and rats, administration of DWCNT by instillation or pharyngeal aspiration resulted in inflammation that lasted up to 6 weeks (rats) to 8 weeks (mice), while mice exposed to DWCNT by inhalation developed inflammation during exposure, but 2 weeks after the termination of exposure the inflammation had resolved. Based on these findings we conducted the present long-term study to assess the chronic toxicity and carcinogenicity of DWCNT in the rat lung.

**Results**

**Interim and terminal sacrifices**

Rats were divided into six groups: no treatment (27 rats); rats administered vehicle alone (30 rats); rats administered 0.125 mg DWCNT (30 rats); rats administered 0.25 mg DWCNT (33 rats); rats administered 0.5 mg DWCNT (30 rats); and rats administered 0.5 mg MWCNT-7 (30 rats). One untreated rat died prior to week 52 and was excluded from the study, therefore, the untreated group contained 26 rats. At week 52 an interim sacrifice was performed on 5 rats from the untreated, vehicle, 0.125 mg DWCNT, and 0.5 mg MWCNT-7 group; 7 rats from the 0.25 mg DWCNT group; and 6 rats from the 0.5 mg DWCNT group. Rats found dead after week 52 underwent terminal necropsy and rats found moribund after week 52 and rats surviving to the end of the study underwent terminal sacrifice. The final terminal sacrifice was performed at 104 weeks on rats from the untreated (17 rats), vehicle (17 rats), 0.125 mg DWCNT (18 rats), 0.25 mg DWCNT (20 rats) and 0.5 mg DWCNT

(16 rats) groups. In the MWCNT-7 group, 16 rats were found moribund or died due to mesothelioma prior to the end of week 90. Therefore, in order to collect pleural lavage fluid the remaining 9 rats in this group underwent final terminal sacrifice at week 91. In addition, in the sixteen MWCNT-7 treated rats that were found moribund or died due to mesothelioma there was extensive invasion of the lungs by the mesotheliomas, making evaluation of proliferative lesion development (other than mesothelioma) in these rats unreliable. Therefore, only the nine MWCNT-7 treated rats that survived for 91 weeks were evaluated for the parameters shown in Table 3. Throughout this report, terminal sacrifice refers to sacrifices performed after week 52 and final sacrifice refers to the terminal sacrifices performed at weeks 91 and 104.

**Characterization of the test substance**

Representative SEM and TEM images of DWCNT and MWCNT fibers in suspension, prior to TIPS administration, are shown in Fig. 1, and fiber lengths and

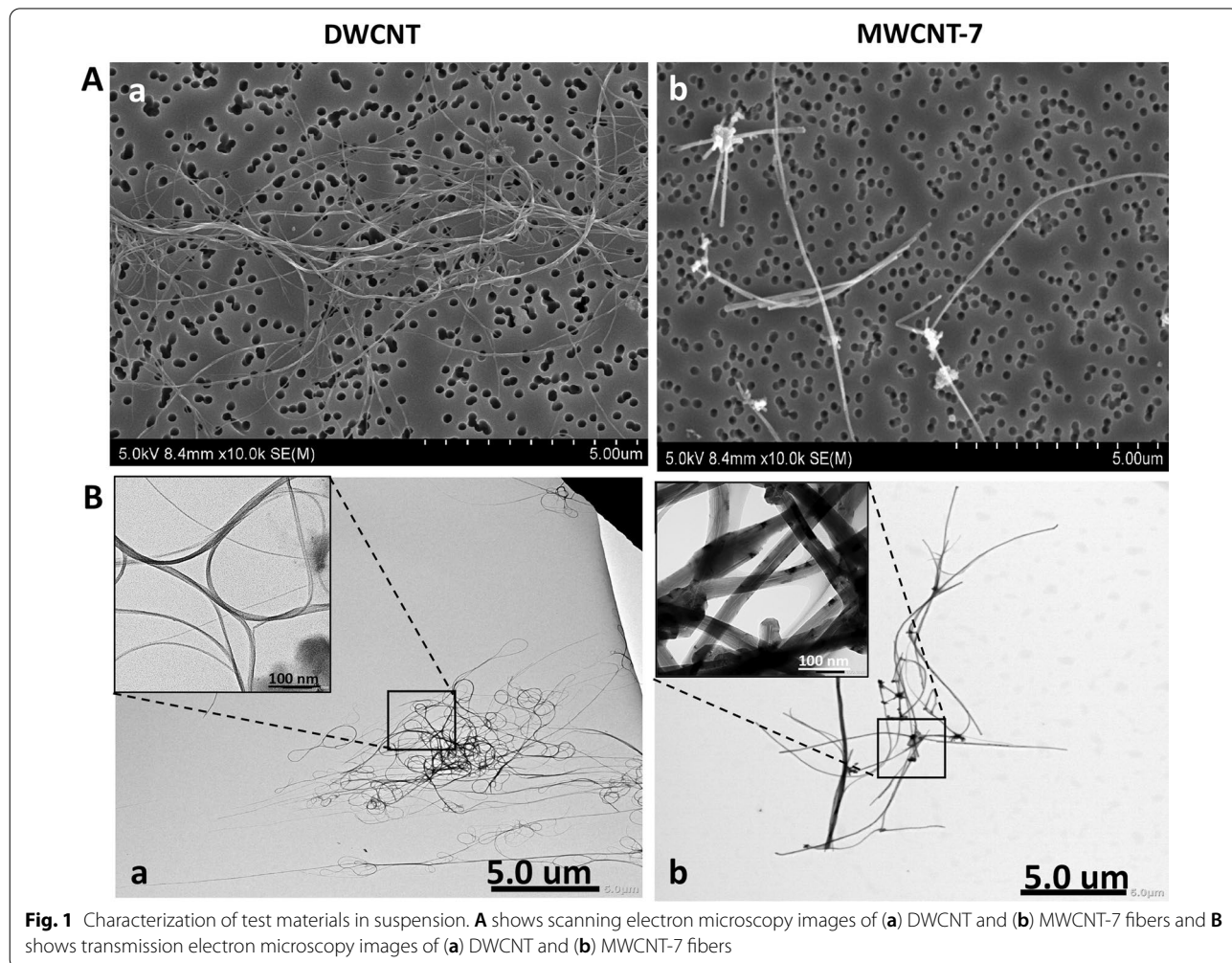


**Fig. 1** Characterization of test materials in suspension. **A** shows scanning electron microscopy images of (a) DWCNT and (b) MWCNT-7 fibers and **B** shows transmission electron microscopy images of (a) DWCNT and (b) MWCNT-7 fibers

diameters are presented in Table 1. DWCNT are thin and tangled and MWCNT are relatively thick and straight. Prior to TIPS administration, DWCNT fibers had a mean diameter of  $14.32 \pm 10.04$  nm, and DWCNT recovered from lung tissue at 104 weeks had a mean diameter of  $15.10 \pm 13.99$  nm. The lengths of the DWCNT fibers could not be measured due to the tangled nature of the fibers. Prior to TIPS administration, MWCNT fibers had a diameter of  $76.49 \pm 31.14$  nm and a mean length of  $8.79 \pm 4.41$   $\mu$ m. MWCNT recovered from lung tissue at 91 weeks had a diameter of  $69.42 \pm 23.76$  nm and a mean length of  $8.45 \pm 5.29$   $\mu$ m. The size of the DWCNT and MWCNT-7 fibers recovered from the lung tissue at 104 weeks and 91 weeks, respectively, was not significantly different from the size of the fibers in suspension prior to TIPS administration.

**Biodegradation of DWCNT and MWCNT-7 in vitro**

DWCNT and MWCNT-7 were added to cultures of RAW cells, a mouse macrophage cell line, or to plates without cells. Plates were then incubated for 5 days. The effective lengths of the DWCNTs incubated without (control) and with RAW cells were estimated using far infrared absorption. The absorption peaks of both samples were observed around  $20\text{ cm}^{-1}$  and the peak shift after incubation was within experimental error: this indicates that the changes in effective length between the controls and the DWCNTs incubated with RAW cells were below detectable limits and that the DWCNTs were not measurably damaged by incubation with RAW cells for 5 days (data not shown).

**Macroscopic findings**

The lungs of rats treated with 0.125, 0.25, and 0.5 mg DWCNT and 0.5 mg MWCNT-7 showed grayish discoloration throughout all lung lobes. The parabronchial and mediastinal lymph nodes of the DWCNT treated rats were dark gray, and the parabronchial and mediastinal lymph nodes of the MWCNT-7 treated rats were entirely black.

**Incidence of proliferative lesions and survival**

No significant differences in the average survival time was observed between the untreated group ( $102 \pm 6$  weeks), the vehicle group ( $99 \pm 10$  weeks), the 0.125 mg/rat DWCNT group ( $99 \pm 8$  weeks), the 0.25 mg/rat DWCNT group ( $101 \pm 7$  weeks), and the 0.5 mg/rat DWCNT group ( $100 \pm 4$  weeks).

Table 2 shows the incidences of proliferative lesions at 52 weeks. No lung tumors were found in any of the rats sacrificed at 52 week. One rat in the MWCNT-7 group developed a malignant pleural mesothelioma. The incidences of bronchioloalveolar hyperplasia (BAH) were significantly higher in the DWCNT 0.25 mg (5/6) ( $p < 0.05$ ) and 0.5 mg (6/7) ( $p < 0.05$ ) groups compared to the vehicle group (0/5). BAH in the DWCNT 0.25 and 0.5 mg groups was also significantly higher ( $p < 0.05$ ) than in the MWCNT-7 group (1/7).

Table 3 shows the incidences of proliferative lesions that developed in the untreated, vehicle, and DWCNT treated rats that survived beyond 52 weeks and in the MWCNT-7 treated rats that survived for 91 weeks: as noted above, the MWCNT-7 rats that died prior to 91 weeks due to mesotheliomas had extensive invasion of the lungs by the mesotheliomas, making

**Table 1** Size of DWCNT and MWCNT-7 fibers in the vehicle before dosing and at weeks 104 and 91

	Length before dosing	Length at 104 & 91 weeks	Diameter before dosing	Diameter at 104 and 91 weeks
DWCNT	NA <sup>a</sup>	NA <sup>a</sup>	$14.32 + 10.04$ nm	$15.10 + 13.99$ nm
MWCNT-7	$8.79 + 4.41$ $\mu$ m	$8.45 + 5.29$ $\mu$ m	$76.49 + 31.14$ nm	$69.42 + 23.76$ nm

<sup>a</sup> Not available (unable to measure DWCNT fiber length because of agglomerate formation)

**Table 2** Incidence of proliferative and neoplastic lesions at 52 weeks

	Untreated	Vehicle	DWCNT 0.125 mg/rat	DWCNT 0.250 mg/rat	DWCNT 0.500 mg/rat	MWCNT 0.500 mg/rat
Number of rats examined	5	5	5	7	6	5
Bronchiolo-alveolar Hyperplasia (BAH)	0	0	2	5* <sup>#</sup>	5* <sup>#</sup>	1
Pleural Mesothelioma	0	0	0	0	0	1

\*Difference from Vehicle group:  $p < 0.05$

<sup>#</sup> Difference from MWCNT-7 group:  $p < 0.05$

No lung tumors were found in any of the rats sacrificed at 52 wk

**Table 3** Incidence of proliferative lesions at the terminal sacrifice<sup>a</sup>

	Untreated	Vehicle	DWCNT 0.125 mg/rat	DWCNT 0.250 mg/rat	DWCNT 0.500 mg/rat	MWCNT 0.500 mg/rat
Rats examined	21	25	25	26	24	9 <sup>a</sup>
Bronchiolo-alveolar hyperplasia (BAH)	4	4	1	4	0	1
Bronchiolo-alveolar adenoma (BAA)	1	1	3	2	3	1
Bronchiolo-alveolar adenocarcinoma (BAC)	0	0	1	2	4	2
BAA + BAC	1	1	4	4	7*	3*
Malignant pleural mesothelioma	0	0	0	1 <sup>b</sup>	1 <sup>b</sup>	0
Malignant peritoneal mesothelioma	0	0	1	0	1	0

<sup>a</sup> In the MWCNT-7 group, 16 animals died from malignant mesothelioma after 52 weeks and before 91 weeks. Because of the invasion of the lungs by the mesotheliomas, these animals could not be accessed for development of BAH, BAA, or BAC or the site of mesothelioma development, and therefore, are not included in Table 3

<sup>b</sup> The malignant pleural mesothelioma developed in the visceral pleura

\* Significantly different from the vehicle group:  $p < 0.05$  and  $0.001$

evaluation of proliferative lesions other than mesothelioma in these rats unreliable. Therefore, only the nine MWCNT-7 treated rats that survived for 91 weeks were evaluated for the parameters shown in Table 3. There was an increase in both bronchioloalveolar adenomas (BAA) and bronchioloalveolar carcinomas (BAC) in the DWCNT groups compared with the vehicle control group. However, the development of carcinomas in the lungs of rats treated with 0.5 mg DWCNT (4/24) was not quite statistically higher ( $p = 0.0502$ ) than the vehicle control group (0/25). On the other hand, the incidence of total lung tumors (BAA + BAC) in the DWCNT 0.5 mg group (7/24) was significantly higher ( $p < 0.05$ ) than the vehicle group (1/25). At the final sacrifice at 91 weeks, three rats had developed lung tumors (BAA + BAC), which has statistical significance compared to the vehicle control group (1/25). The incidence of malignant pleural mesothelioma in the MWCNT-7 group (16/25) was significantly higher ( $p < 0.001$ ) than the vehicle group (0/25); this is not shown in Table 3. One rat in the 0.25 mg DWCNT group and one rat in the 0.50 mg DWCNT group also developed mesotheliomas, however, both of these mesotheliomas developed in the visceral pleura and as discussed below are unlikely to be relevant to human mesothelioma development. Two rats, one in the 0.125 mg DWCNT group and one in the 0.50 mg DWCNT group, also developed malignant peritoneal mesotheliomas, however, aged male Fischer 344 rats are prone to developing spontaneous peritoneal mesotheliomas [31]. Figure 2 shows typical lesions that developed in these rats. Other tumors including leukemia, pituitary tumors, mammary tumors, and scrotal malignant mesotheliomas were not treatment related.

### Histopathological evaluation

Table 4 shows pathological parameters at 52 weeks and Table 5 shows pathological parameters at the final sacrifice. Histopathological observation at 52 weeks and at the final sacrifice showed that DWCNTs were mostly phagocytosed by groups of macrophages forming foreign body granulation tissue (Fig. 3), and at both time points granulation tissue was significantly increased in all treated groups compared to the vehicle group. Granulation tissue was also significantly higher in the DWCNT 0.25 and 0.5 mg groups compared to the MWCNT-7 group at week 52 and in the DWCNT 0.5 mg group compared to MWCNT-7 group at the final sacrifice. In contrast to DWCNT, MWCNT-7 fibers were commonly observed in free macrophages and some fibers were observed free in the alveolar space (Fig. 3). Both DWCNT and MWCNT-7 fibers were found in the parabronchial and mediastinal lymph nodes (Fig. 4).

Immunohistochemical evaluation showed that at 52 weeks and at the final sacrifice, the CD68 positive macrophage count was significantly increased in all treated groups compared with the vehicle group (Tables 4 and 5). The macrophage count was also significantly increased in the DWCNT 0.25 and 0.5 mg groups compared to the MWCNT-7 group at both time points. Figure 5A shows CD68 immunostaining of vehicle, 0.5 mg DWCNT, and 0.5 MWCNT-7 lungs at the final sacrifice.

PCNA indices in the lung at 52 weeks are shown in Table 4. PCNA indices of alveolar cells in the rats administered DWCNT were not different from the controls at week 52. In contrast, PCNA indices of alveolar cells in the rats administered MWCNT were significantly increased compared to the controls at week 52.

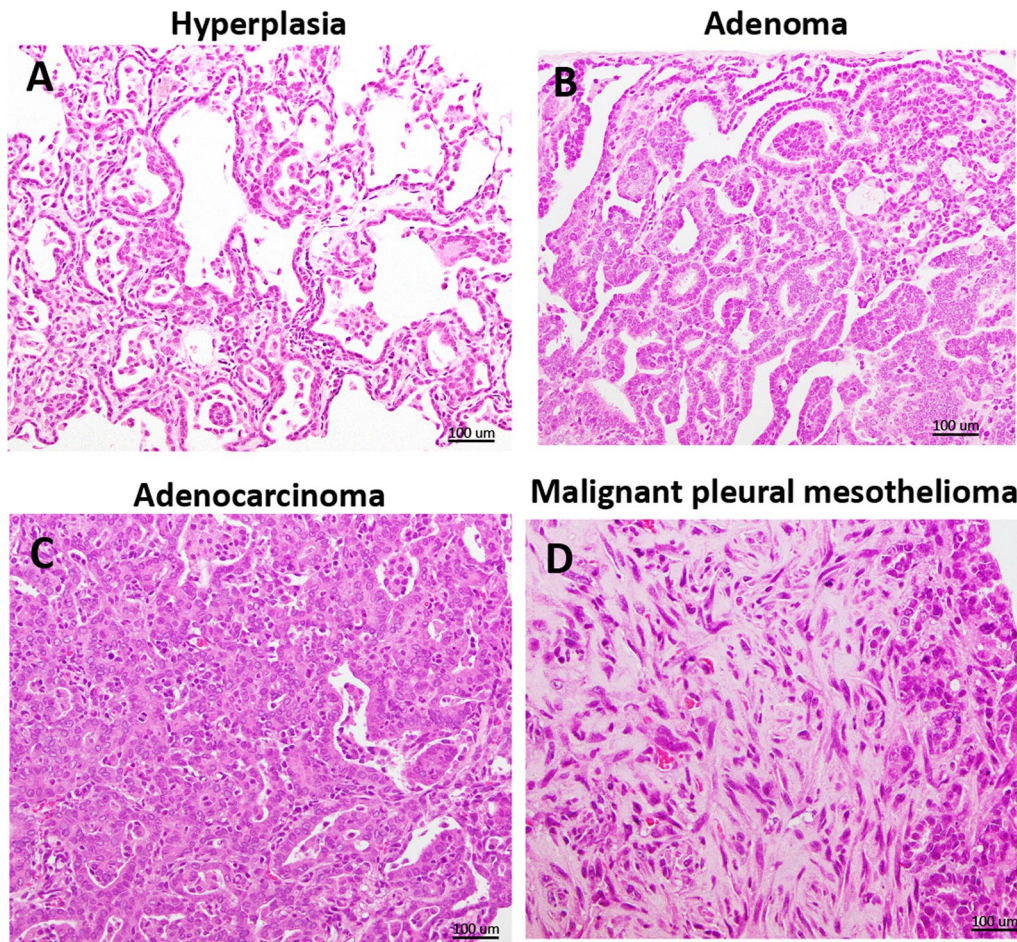


**Fig. 2** Representative preneoplastic and neoplastic lesions. **A** Bronchiolo-alveolar hyperplasia, **B** Bronchiolo-alveolar adenoma, **C** Bronchiolo-alveolar adenocarcinoma, and **D** Malignant pleural mesothelioma

**Table 4** Cell proliferation and inflammation related parameters in the lung tissue at 52 weeks

	Untreated	Vehicle	DWCNT 0.125 mg/rat	DWCNT 0.250 mg/rat	DWCNT 0.500 mg/rat	MWCNT 0.500 mg/rat
Granulation tissue count/cm <sup>2</sup> mean ± S.D	1.1 ± 0.35	2.4 ± 1.2	98.8 ± 31.0***	189 ± 32.5***,#	404.4 ± 88.8***,#	65.4 ± 11.8**
Macrophage count/cm <sup>2</sup> mean ± S.D	1.45 ± 0.23	6.93 ± 1.47	21.72 ± 4.2***	33.01 ± 6.4***,#	49.1 ± 5.79***,#	15.88 ± 5.79**
Alveolar cell PCNA index %	10.77 ± 3.00	18.10 ± 8.65	16.51 ± 7.85	17.81 ± 7.40	25.85 ± 4.74	44.52 ± 7.55 **
CCL2 pg/mg lung protein mean ± S.D	3.30 ± 0.28	3.65 ± 0.44	16.69 ± 4.65***	23.36 ± 4.33***,#	22.37 ± 3.7***,#	9.49 ± 0.98***
CCL3 pg/mg lung protein mean ± S.D	6.82 ± 0.56	8.19 ± 0.73	40.32 ± 10.4**	69.09 ± 7.84***,#	135.57 ± 11***,#	24.86 ± 8.4*

\*, \*\*, \*\*\*Difference from the Vehicle group at p < 0.05, 0.01, 0.001, respectively  
 #, ## Significantly increased compared to MWCNT-7 at p < 0.05, 0.01 respectively

PCNA indices at the final sacrifice are shown in Table 5 and Fig. 5B shows PCNA immunostaining of vehicle, 0.5 mg DWCNT, and 0.5 MWCNT-7 lungs at the final sacrifice. The PCNA index of alveolar cells was

significantly increased in all treated groups compared with the vehicle group. The visceral and parietal pleural mesothelial PCNA indices were not increased in any of the DWCNT groups compared to the controls. The

**Table 5** Cell proliferation and inflammation related parameters of the lung tissue at the final sacrifice<sup>a</sup>

	Untreated	Vehicle	DWCNT 0.125 mg/rat	DWCNT 0.250 mg/rat	DWCNT 0.500 mg/rat	MWCNT <sup>a</sup> 0.500 mg/rat
Granulation Tissue count/cm <sup>2</sup> mean ± S.D	0.9 ± 0.3	1.3 ± 0.6	50.9 ± 5.2**	118.9 ± 68.8***	365.1 ± 81.7***, #	94.9 ± 35.3**
Macrophage count/cm <sup>2</sup> mean ± S.D	54.6 ± 16.4	75 ± 23.0	361.8 ± 53.4***	502.8 ± 59.1***, #	479.1 ± 48.2***, #	314.7 ± 91.6***
Alveolar PCNA index %	3.62 ± 1.7.3	4.48 ± 1.88	8.83 ± 4.28*	18.54 ± 7.35**	21.27 ± 10.57***, #	14.10 ± 10.29**
Visceral pleural PCNA index %	0.20 ± 0.28	0.36 ± 0.26	0.44 ± 0.17	1.40 ± 1.23	1.32 ± 0.72	15.20 ± 13.22*** <sup>§</sup>
Parietal pleural PCNA index %	2.00 ± 0.43	2.30 ± 0.66	2.00 ± 0.712	1.90 ± 0.77	2.60 ± 0.28	23.75 ± 32.56*** <sup>§</sup>
Pulmonary Collagen deposition % <sup>b</sup>	13.04	8.50	13	18.15	20.47*	27*
Subpleural Collagen deposition % <sup>c</sup>	4.20	2.25	5.50	4.45	16.87	64.20*** <sup>§</sup>
CCL2 ng/mg lung protein mean ± S.D	0.77 ± 0.3	1.6 ± 0.87	6.67 ± 2.44***	8.40 ± 1.73***, #	10.74 ± 1.94***, #	5.20 ± 1.6***
CCL3 ng/mg lung protein mean ± S.D	0.58 ± 0.27	0.55 ± 0.16	0.71 ± 0.16*, #	0.75 ± 0.21*, #	0.74 ± 0.19*, #	0.52 ± 0.12

<sup>a</sup> In the MWCNT-7 group, 16 animals died from malignant mesothelioma after 52 weeks and before 91 weeks. Because of the extensive invasion of the lungs by the mesotheliomas, these animals could not be assessed for the parameters shown in Table 5. Therefore, only the values obtained from the nine MWCNT-7 treated rats that survived for 91 weeks are shown in Table 5

<sup>b</sup> Results are expressed as the percentage area of pulmonary collagen deposition/total alveolar tissue area

<sup>c</sup> Results are expressed as the percentage area of subpleural collagen deposition/total pleural tissue area

\*\*\*, \*\*\*\* Significantly increased from the Vehicle at  $p < 0.05$ ,  $0.01$ ,  $0.001$  respectively

#, ## Significantly increased compared to MWCNT-7 at  $p < 0.05$ ,  $0.01$  respectively

<sup>§</sup> Significantly increased in compared to DWCNT groups:  $p < 0.01$

visceral and parietal pleural mesothelial PCNA indices were significantly higher in the MWCNT-7 group compared to the vehicle group and to the DWCNT groups.

Pulmonary collagen deposition at the final sacrifice is shown in Table 5, and Fig. 5C shows Masson's trichrome staining of vehicle, 0.5 mg DWCNT, and 0.5 MWCNT-7 lungs at the final sacrifice. Fibrotic changes with increased deposition of collagen in the alveolar wall, parabronchial areas, and within the granulation tissues were observed in the DWCNT and MWCNT-7 groups. Pulmonary collagen deposition was significantly higher in the 0.5 mg DWCNT and MWCNT-7 groups compared to the vehicle control group.

Subpleural collagen deposition at the final sacrifice is shown in Table 5, and Fig. 6 shows Masson's trichrome collagen staining of visceral and parietal pleura. Subpleural collagen deposition was somewhat increased in the visceral pleura but not in the parietal pleura of the 0.5 mg DWCNT group, and overall subpleural collagen deposition was not significantly increased in the 0.5 mg DWCNT group compared to the controls. MWCNT-7 treated rats had increased collagen deposition at both the visceral and parietal pleura, and overall subpleural collagen deposition was significantly higher in the MWCNT-7 group than the vehicle controls and the 3 DWCNT groups.

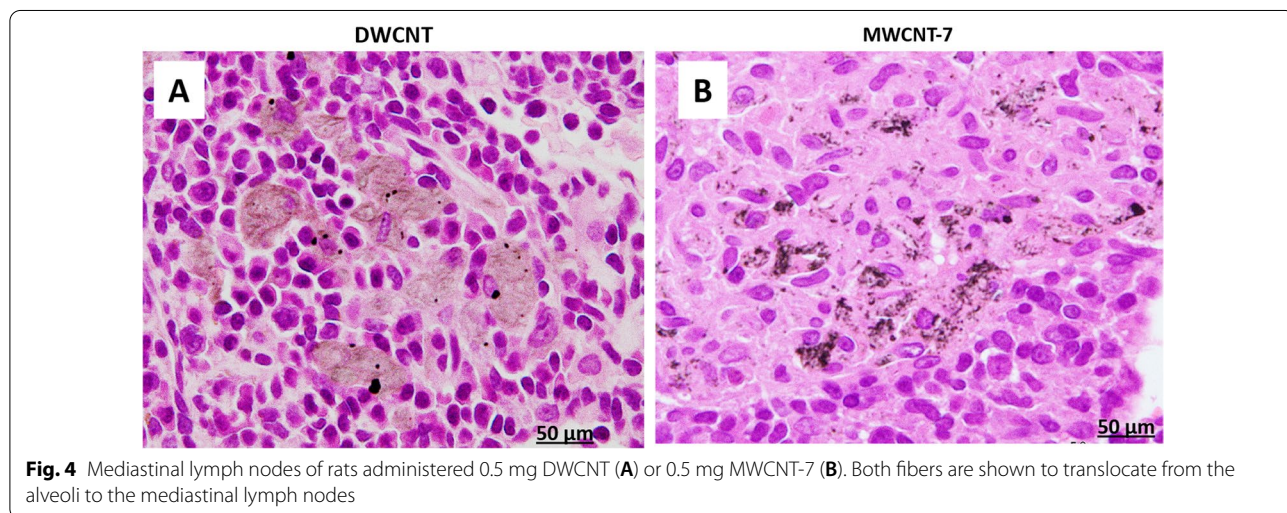
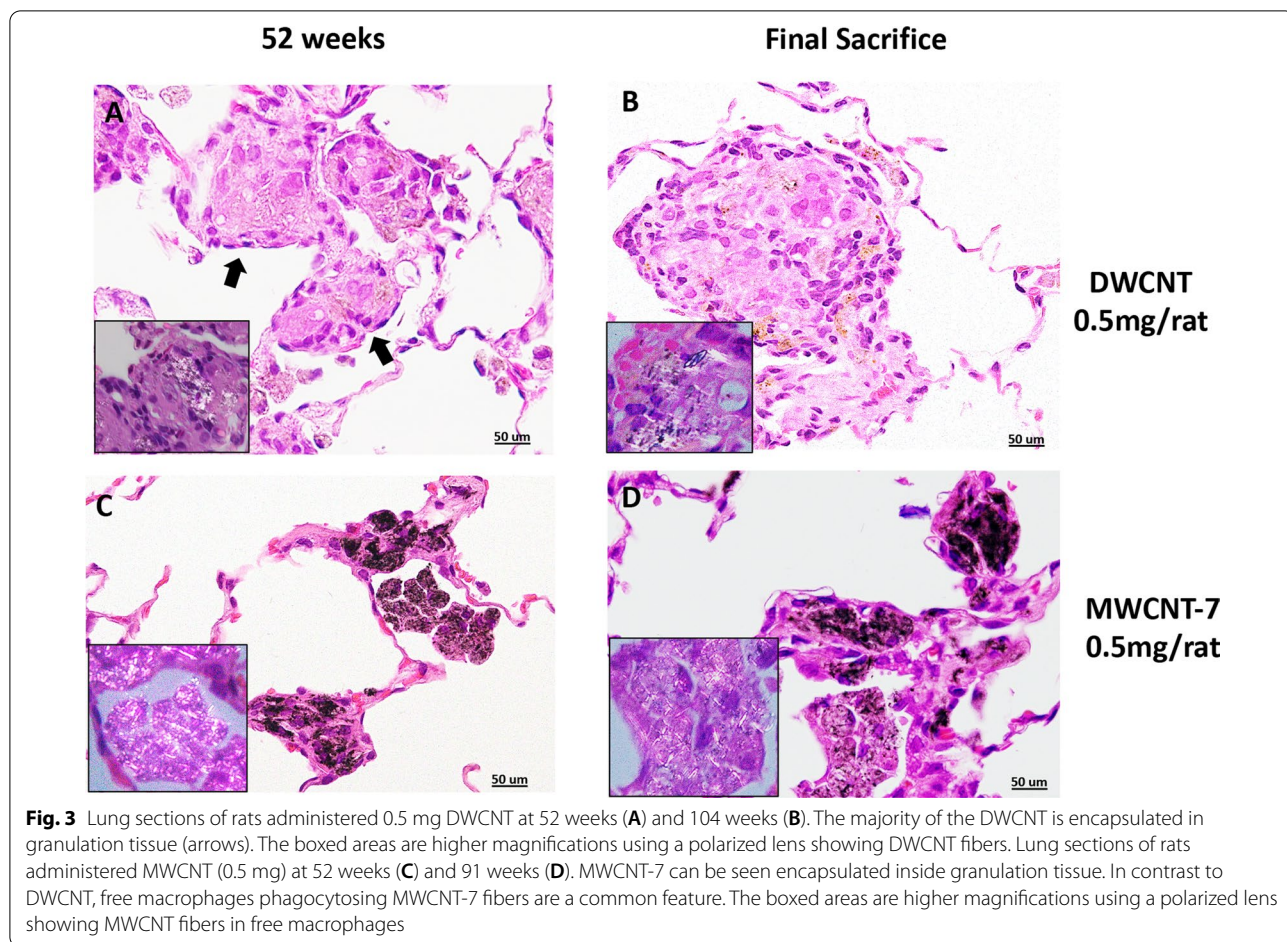
The levels of CCL2 and CCL3 in lung tissue at 52 weeks and the final sacrifice are shown in Tables 4 and 5. The levels of both CCL2 and CCL3 in lung tissue at both 52 weeks and the final sacrifice were significantly higher in all treated groups compared with the vehicle control group. The CCL2 and CCL3 levels in the DWCNT 0.25 and 0.5 mg groups were significantly higher than the MWCNT-7 group at both 52 weeks and at the final sacrifice.

#### Lung fiber burden at 52 weeks and the final sacrifice

The lung fiber burden at 52 weeks and the final sacrifice is shown in Fig. 7. At 52 weeks, the amounts of DWCNTs in the lungs were proportional to the initial dose administered. Lung fiber burden decreased from week 52 to the final sacrifice, however, more than 1% of the initially instilled fibers remained in the lung 104 weeks and 91 weeks after instillation of DWCNT and MWCNT-7, respectively, and both DWCNT and MWCNT-7 were readily detectable in lung tissue sections at the final sacrifice (see Figs. 3 and 5), indicating that DWCNT as well as MWCNT-7 was biopersistent in the rat lung.

#### Electron microscopic observation

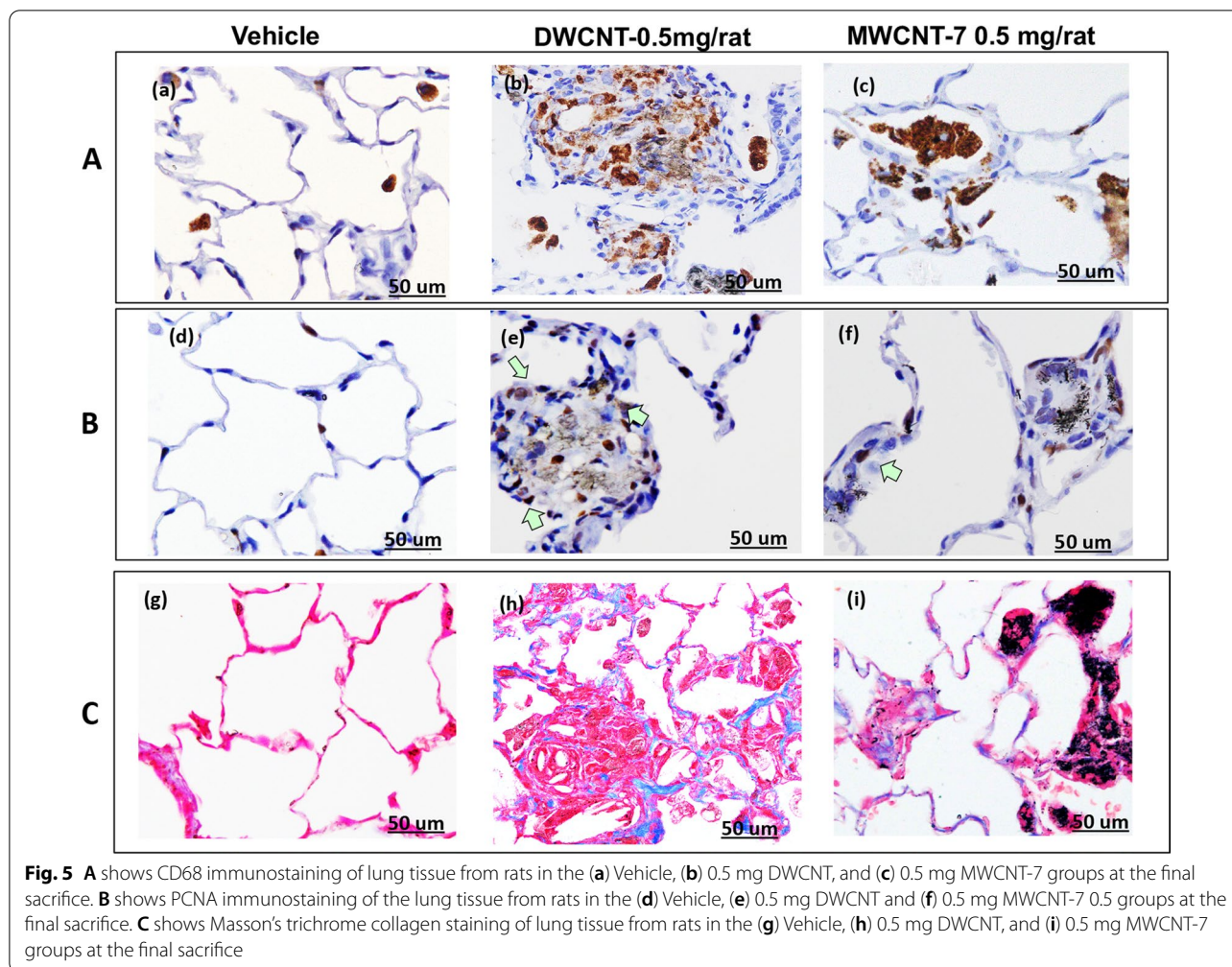
At 104 weeks, DWCNT agglomerates were mostly found engulfed by groups of macrophages forming granulation



tissue with multinucleated giant cells (Fig. 3). Figure 8 is a TEM image of irregular tangled DWCNT fibers in a multinucleated giant cell. Figure 9 is an SEM image of numerous thin DWCNT fibers engulfed by a

single macrophage. In contrast, TEM and SEM images of MWCNT-7 treated rats sacrificed at 91 weeks primarily showed single MWCNT-7 fibers or small bundles of MWCNT-7 fibers associated with macrophages (Figs. 8





and 9). MWCNT-7 fibers were also found free in the alveolar space (Fig. 9). Importantly, MWCNT-7 fibers could also be seen penetrating the macrophage cell membrane (Fig. 9).

#### DNA adductomes formation in the lung tissue

Additional file 1: Fig. S1 shows adductome maps of rats at 52 weeks. The relative peak areas and the number of peaks are given for each group. There were no significant differences in either peak area or the number of peaks between any of the groups. No adducts specific to any of the treated groups were found.

#### HMGB1 levels in the pleural lavage fluid at the final sacrifice

HMGB1 is a serum marker for mesothelioma [32–35]. HMGB1 is released from mesothelial cells when they undergo necrosis induced by exposure to asbestos fibers [32, 36], and the released HMGB1 is involved in malignant transformation [34, 36–39]. Therefore, the

PLF of rats with malignant mesothelioma is expected to contain elevated levels of HMGB1. At the final sacrifice, the PLF levels of HMGB1 were not elevated in the DWCNT treated rats, but were significantly elevated ( $p < 0.001$ ) in the MWCNT-7 treated rats (Fig. 10): untreated ( $0.34 \pm 0.08$  ng/ml), vehicle ( $0.43 \pm 0.24$  ng/ml), 0.125 mg DWCNT ( $0.35 \pm 0.12$  ng/ml), 0.25 mg DWCNT ( $0.30 \pm 0.09$  ng/ml), 0.5 mg DWCNT ( $0.71 \pm 0.48$ ), and 0.5 mg MWCNT-7 at 91 weeks ( $1.91 \pm 1.19$  ng/ml). Notably, HMGB1 levels were not elevated the pleural lavage fluid of the 0.5 mg DWCNT treated rat that developed visceral pleural mesothelioma (0.52 ng/ml); the rat treated with 0.25 mg DWCNT that developed visceral pleural mesothelioma was found dead and therefore pleural lavage fluid could not be collected from this rat. As discussed below, the pleural mesotheliomas that developed in the DWCNT treated rats are unlikely to be relevant to human mesothelioma development.

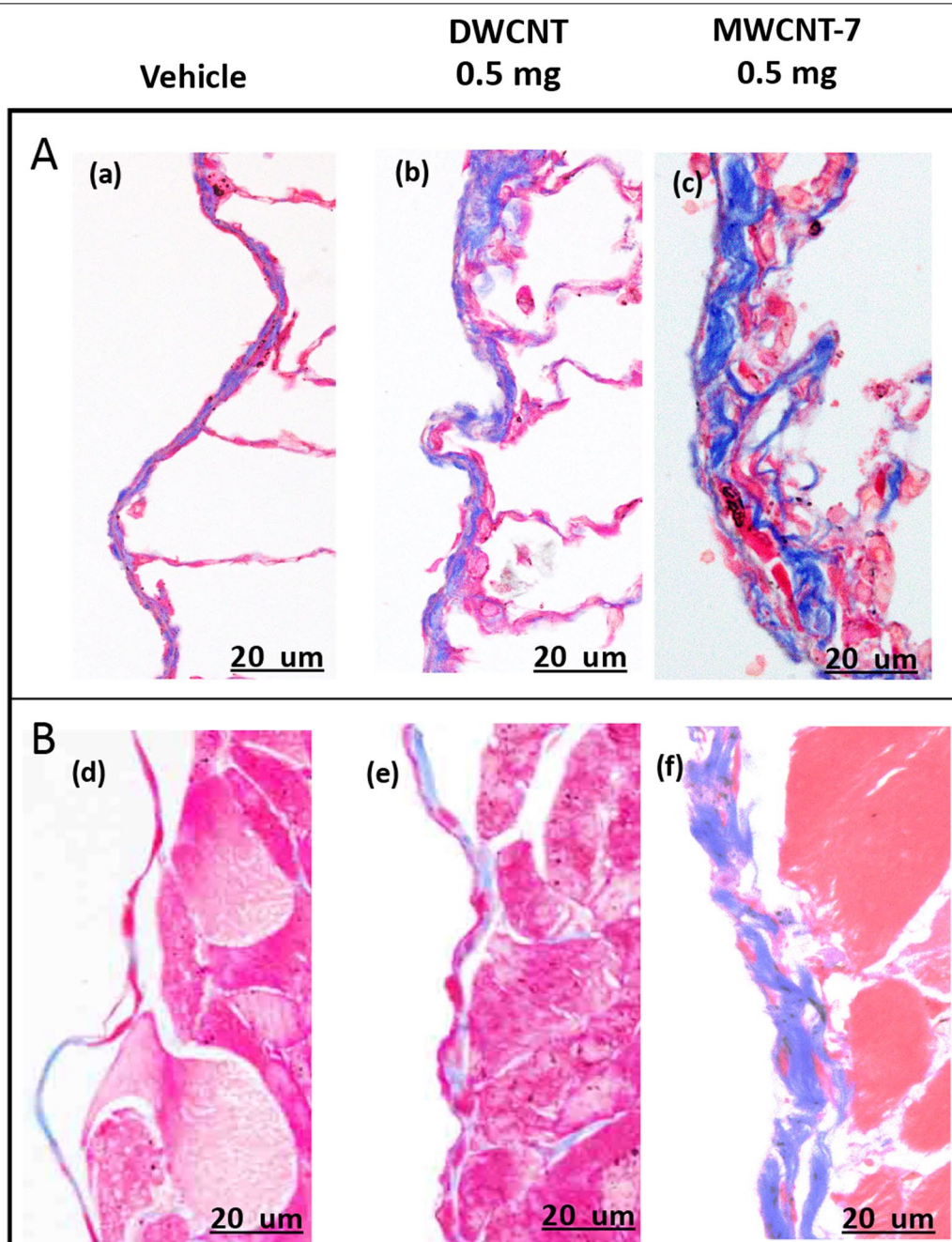
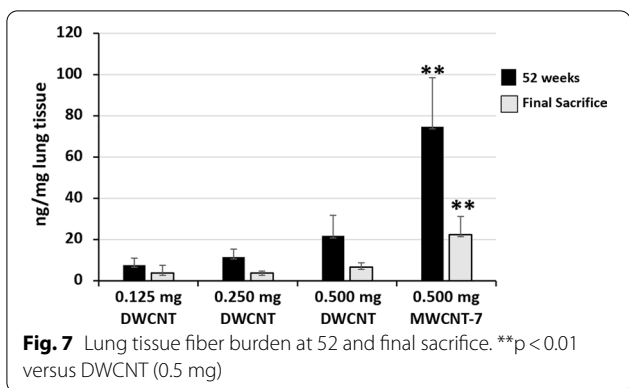


**Fig. 6** **A** shows Masson's trichrome collagen staining of the visceral pleura of rats from the (a) Vehicle, (b) DWCNT 0.5 mg, and (c) MWCNT-7 0.5 mg groups at the final sacrifice. Panel **B** shows Masson's trichrome collagen staining of the parietal pleura of rats from the (a) Vehicle, (b) DWCNT 0.5 mg, and (c) MWCNT-7 0.5 mg groups at the final sacrifice

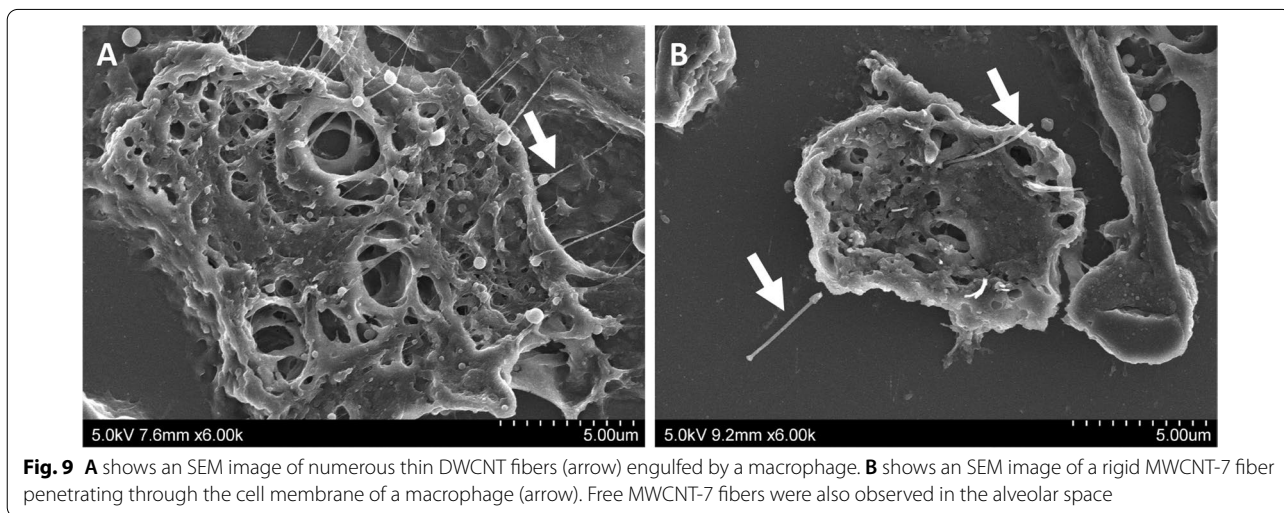
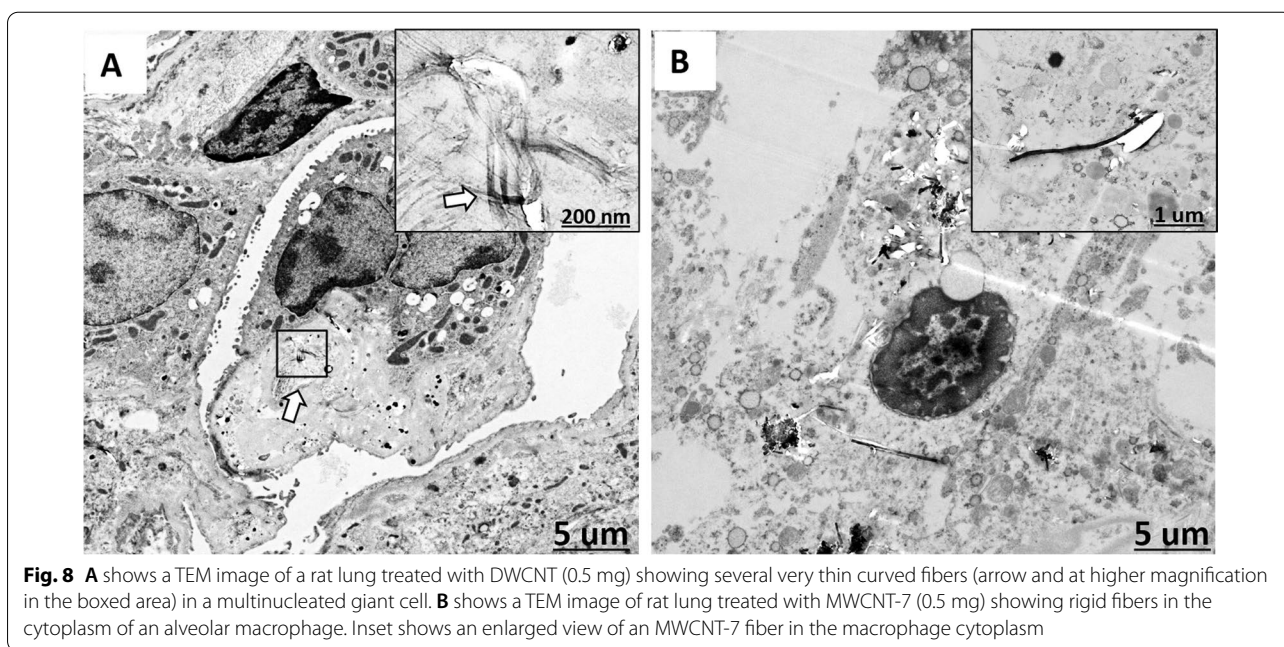
### Discussion

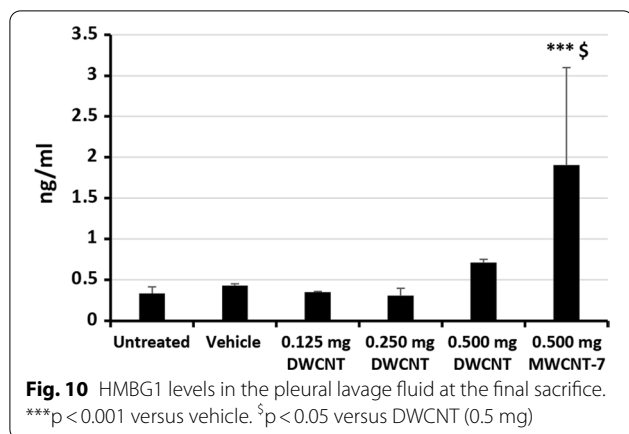
This is the first long-term, 2-year in vivo study to assess the toxicity and carcinogenicity of DWCNTs in the rat lung. Rats were untreated or administered vehicle or 0.125 mg, 0.25 mg, or 0.5 mg DWCNT per rat or 0.50 mg MWCNT-7 per rat: MWCNT-7 was used as the

reference material. We found that DWCNTs were bio-persistent in the rat lung and induced chronic inflammation, and that the 0.50 mg group developed lung fibrosis and lung tumors (see Tables 1, 3, and 5). At 52 weeks, rats in the 0.25 mg and 0.50 mg groups had significantly elevated levels of hyperplasia in the lung, and at



104 weeks one rat in the 0.125 mg DWCNT group, 2 rats in the 0.25 mg DWCNT group, and 4 rats in the 0.50 mg DWCNT group had developed adenocarcinomas (see Tables 2 and 3). While these incidences were not statistically significant compared to the vehicle controls, which did not develop adenocarcinomas, the apparent dose response agrees with the possibility that in this study the DWCNT fibers that were tested may have had carcinogenic potential. In addition, the incidence of total lung tumors, bronchiolo-alveolar adenoma and bronchiolo-alveolar carcinoma combined, was significantly higher in the 0.5 mg DWCNT group compared to the vehicle





controls (see Table 3). Overall, these results indicate that the possibility that DWCNTs are carcinogenic cannot be ignored and that further long-term studies to assess the in vivo toxicity and carcinogenicity of DWCNT should be carried out.

It is notable that two rats administered DWCNT developed malignant pleural mesothelioma (see Table 3). The development of this tumor is rare in rats: the Japan Bioassay Research Center historical control data shows that approximately 1 of 1000 rats spontaneously develop malignant pleural mesothelioma and a retrospective review by Tokarz et al., 2021, identifies spontaneous primary pleural mesothelioma developing in approximately 1 of 2000 male F344 rats [40]. This suggests that development of these tumors is biologically significant. However, the PLF of the rats administered DWCNT did not have elevated levels of HMGB1. In contrast, the PLF of the rats administered MWCNT-7 did have elevated levels of HMGB1 (see Fig. 10). HMGB1 is released from mesothelial cells when they undergo necrosis induced by exposure to asbestos fibers [32, 36], and the released HMGB1 is involved in malignant transformation [34, 36–39], suggesting that rats developing fiber-associated pleural mesothelioma would be expected to have elevated levels of HMGB1 in their PLF. In addition, HMGB1 is a serum marker for mesothelioma in humans [32–35], suggesting that HMGB1 is also released from cells in patients with advanced mesothelioma. Therefore, the PLF of rats with either developing or advanced malignant pleural mesothelioma would be expected to contain elevated levels of HMGB1, as is the case for the rats administered MWCNT-7. The absence of elevated levels of HMGB1 in the groups administered DWCNT suggests that these lesions were not associated with fibers in the pleural cavity. Another notable point is that the pleural mesotheliomas that developed in the DWCNT administered rats developed in the visceral pleural. Fiber-associated pleural

mesotheliomas are induced by fibers that are retained in the pleural cavity. These fibers are retained at the parietal pleura as they are carried by the pleural fluid that flows out of the pleural cavity through the stomata present in the parietal pleura, and consequently, fiber-associated pleural mesotheliomas initially develop in the parietal pleura [41–46]. This also suggests that development of visceral mesothelioma in the DWCNT administered rats was not due to DWCNT fibers present in the pleural cavity. Finally, it is well known that the visceral pleura in rats is thin, consisting of the pleural mesothelial layer and a basement membrane lying directly over the alveoli (see Fig. 6A), while in humans the visceral pleura has substantial submesothelial connective tissue. Consequently, in rats, but not in humans, interactions occurring in the lung alveoli adjacent to the visceral pleura could affect visceral pleural mesothelial cells, making the mechanism of visceral mesothelioma induction in rats not applicable to humans. Therefore, development of pleural mesothelioma in the visceral pleura coupled with the absence of elevated levels of HMGB1 in the PLF of the rats administered DWCNT support the premise that development of pleural mesothelioma in the DWCNT treated rats in the current study is not biologically relevant to humans.

Two rats also developed malignant peritoneal mesothelioma. However, aged male Fischer 344 rats are prone to developing spontaneous peritoneal mesotheliomas [31]. Therefore, the low incidence of these mesotheliomas suggests that they are not treatment related.

Another notable result in the present study is the apparently low incidence of lung tumors in the MWCNT-7 treated rats: 2 rats developed lung carcinomas and 1 rat developed a lung adenoma. However, it needs to be noted that 16 rats in this group died before the end of the study due to mesotheliomas, and therefore, the incidence of lung tumor development in rats surviving to the final sacrifice of this group of animals at 91 weeks (9 rats) was numerically higher than in the DWCNT groups. Notably, an incidence of 2 carcinomas and 3 lung tumors in 9 rats is identical to the incidence of carcinomas and lung tumors in a two year inhalation study by Kasai et al. [17]. In the Kasai et al. study, 11 carcinomas and 16 lung tumors developed in 50 male rats exposed to 2 mg/m<sup>3</sup> MWCNT-7 for 2 years. A low incidence of lung tumor development (0 rats) accompanied by a high incidence of mesothelioma development was also observed in a previous study in which rats administered MWCNT-7 by TIPS died before the end of the study period due to mesothelioma [20]. Therefore, tumor development in rats treated with MWCNT-7 in the present study was similar to that reported previously.

The DWCNT fibers used in the present study formed tangled agglomerates: agglomerate is used as defined

by Walter 2013 [47]. Agglomerate formation is a known characteristic of CNTs [48, 49]. In the atmosphere of the working environment, CNTs are usually found as aggregates or agglomerates and rarely as single fibers [2, 50]. DWCNT agglomerates deposited beyond the ciliated airways were not completely moved out of the lung or broken down by alveolar macrophages (see Table 1 and Fig. 7). It is well known that persistence of CNTs in the lung induces inflammation [2, 48, 49, 51, 52]. In our earlier study, at 6 weeks after administration of DWCNT to rats mild inflammation was observed and granulomas, which are an inflammatory sequestration response [53, 54], containing DWCNT fibers had developed [30]. In the present study, biopersistence of the DWCNT fibers in the rat lung induced persistent inflammation: at 52 and 104 weeks macrophage count, CCL2 and CCL3 expression, and granuloma formation was significantly elevated in the lungs of all DWCNT treated rats (Tables 4 and 5). Chronic inflammation is a hallmark of cancer [55–58] and at 52 weeks hyperplasia was observed in the lungs of the 0.25 and 0.50 mg DWCNT treated rats and at 104 weeks the alveolar PCNA index was elevated in all DWCNT treated rats and tumor incidence was significantly increased the rats administered 0.5 mg DWCNT.

Fibrosis is characterized by the excess accumulation of the extracellular matrix (ECM) in response to non-resolving chronic inflammation [51, 52, 59–61]. Pulmonary fibrosis can impair lung function resulting in morbidity and mortality in humans [51, 59, 62]. During the chronic response to biopersistent CNTs, granulomas containing CNTs and characterized by local accumulation of activated macrophages serve as fibrogenic foci [59]. In our study, at 52 and 104 weeks all three groups of DWCNT treated rats had significant amounts of granulation tissue, increased macrophage counts, and elevated levels of CCL2 and CCL3, indicating the presence of activated macrophages, in the lung. Figure 5 shows collagen deposition at the fibrogenic foci formed by granulomas containing DWCNT and MWCNT-7 fibers. At 104 weeks elevated collagen deposition in the lung was observed in rats administered 0.25 and 0.50 mg DWCNT, and in the rats administered 0.50 mg DWCNT collagen deposition was significantly higher than the vehicle controls. In addition, fibrosis can be associated with tumorigenesis [52, 63], and in our study, the rats administered 0.50 mg DWCNT had significantly elevated collagen deposition and a significantly increased tumor incidence.

An important point regarding the results of the present study is how DWCNT can be tumorigenic in the rat lung but thin tangled CNTs do not induce the development of mesotheliomas, even when injected into the peritoneal cavity at relatively high levels [18, 19, 21]. One likely factor is the reported role of HMGB1 in the development

of mesotheliomas [34, 36–39]. Interaction of rigid fibers with mesothelial cells can result in cytotoxicity and release of HMGB1 from the cell, and the released HMGB1 can promote malignant transformation [34, 36–39]. In contrast, thin tangled CNTs are reported to be less cytotoxic to mesothelial cells [64], and consequently, thin tangled fibers could be considerably less carcinogenic to mesothelium than rigid fibers.

As discussed above, the DWCNT fibers used in this study displayed characteristics typical of biopersistent fibers. As it is highly likely that individual DWCNT fibers would be phagocytosed and removed from the lung by alveolar macrophages, the biopersistence and subsequent induction of chronic inflammation, fibrosis, and tumorigenesis were the result of the agglomerates formed by the fibers. Since CNTs are typically found as aggregates of agglomerates and not as single fibers in the workplace [2], agglomerate formation by the DWCNT fibers used in the present study is not unexpected. Therefore, this characteristic must be taken into consideration when assessing the toxicity of CNTs, especially thin CNTs.

Occupational exposure to CNTs range from less than  $1 \mu\text{g}/\text{m}^3$  to several  $\mu\text{g}/\text{m}^3$  [65–68]. Using an exposure of  $1 \mu\text{g}/\text{m}^3$ , and an alveolar surface area of  $0.4 \text{ m}^2$  for a Fisher 344 rat and  $102 \text{ m}^2$  for a human [69] and a 7% deposition rate in humans (Figs. 6–6 & 6–7 [70]) a human would have to inhale 1,820 mg DWCNT to acquire the same DWCNT burden as a rat instilled with 0.5 mg DWCNT. Given a minute ventilation rate of 20 L/min for a human doing light work ([https://doi.org/10.1016/0273-2300\(92\)90040-G](https://doi.org/10.1016/0273-2300(92)90040-G)), in an environment containing  $1 \mu\text{g}/\text{m}^3$  DWCNT, 1,820,000  $\mu\text{g}$  DWCNT would be inhaled by an unprotected human worker in approximately 91,050,000 min or approximately 1,517,500 h. This is obviously much longer than a working lifetime. However, the lung toxicities of fibers differs in rats and humans. For asbestos, the only type of fiber for which a direct comparison can be made for lung toxicities of rats and humans, the lung tissue burden of crocidolite asbestos that caused a carcinogenic response in rats (1250 fg/ $\mu\text{g}$  dry lung tissue weight) was 6000 times higher than in humans (0.2 fg/ $\mu\text{g}$  dry lung tissue weight) [71, 72]: it is reasonable that rats have stronger lung defenses to dusts than humans as rats are exposed to dusts much more than humans and short-lived rats will be exposed to fibers for a much shorter period than long-lived humans allowing rats to tolerate much higher fiber loads than humans. This difference in the carcinogenic response of rats and humans to respired fibers suggests that it is possible for a worker to inhale a potentially toxic level of DWCNT in the workplace. Notably, the 2013 report by the national Institute for Occupational safety and Health Current Intelligence Bulletin 65 states that given the

known adverse respiratory effects of CNTs in animals, all types of CNT and CNF (carbon nanofibers) should be considered an occupational respiratory hazard (see Sect. 4 Conclusions—Hazard and Exposure Assessment in [73]).

One limitation of the present study is that poorly soluble particles (PSPs) of low toxicity can have toxic effects in the rat lung. Toxic effects occur when pulmonary macrophage clearance of the particles is impaired due to an excessive particle load in the lung; impaired clearance due to an excessive particle load is known as particle overload and the condition is known as lung overload. However, instillation of 0.5 mg PSPs into the rat lung does not result in an excessive particle load in the lung. For example, administration of 0.5 mg of rutile-type nano TiO<sub>2</sub> (r-nTiO<sub>2</sub>) particles by TIPS did not result in particle overload in the rat lung: rats administered 0.25 mg and 0.5 mg r-nTiO<sub>2</sub> by TIPS did not develop any lesions or clinical signs related to the instilled particles [74]. However, in that study the r-nTiO<sub>2</sub> was cleared from the lungs while in the present study, the DWCNT fibers were not cleared from the lungs. Therefore, it is possible that biopersistence of DWCNT in the rat lung could be viewed as particle overload. Another point concerning particle overload is that the mechanism associated with the toxic effects mediated by particle overload are chronic inflammation, fibrosis, and tumorigenesis [75], and this mechanism is the same mechanism by which fibers generate toxic effects in the lung (summarized in Fig. 4.2 in [10]). One proposal regarding particle overload in rats and humans is that in humans, but not rats, particles are transferred into interstitial sites where they do not interact with macrophages, thereby averting chronic inflammation, fibrosis, and tumorigenesis (Fig. 4 in [75]). However, interstitialisation of PSPs may not apply to DWCNT agglomerates. A defining characteristic of particle overload induced tumorigenesis is that it is generally specific to rats [75]. Therefore, to further investigate the toxicity and carcinogenicity of DWCNT in the lung, toxicity and carcinogenicity of DWCNT needs to be assessed using a second test animal, such as mice, [76]: Notably, IARC accepts evidence of tumorigenicity in two animal species as sufficient evidence of carcinogenicity in experimental animals [77].

The present study has two other limitations. While we show that the possibility that respired DWCNT is a toxic to humans cannot be ignored, our study does not have unambiguous evidence that the DWCNT fibers we tested are carcinogenic in rats. However, after demonstrating the possibility that DWCNT fibers are toxic to the rat lung, a future study with a larger number of animals in the DWCNT groups can be performed. The third limitation is that administration of a test substance

by instillation can be used for hazard identification and hazard ranking, but instillation cannot be used for risk characterization [78]. Therefore, if DWCNTs are identified as toxic in experimental animals, inhalation studies to characterize DWCNT risk need to be done.

Importantly, the response of the rat lung to particle overload should not be interpreted as indicating that the rat is not suitable for use in inhalation studies that test the toxicity of respirable particles. As stated by Bos et al., 2019, "Unless available data clearly point out otherwise, rat pulmonary toxicity including lung inflammation and tumour formation, needs to be considered relevant for human hazard and risk assessment" [79].

A final point regarding this study is how instillation studies using rats compare with inhalation studies. Instillation bypasses the upper respiratory tract, allowing pulmonary deposition of test material without nasal filtering, and instillation delivers a high amount of the test material to the lungs as a single bolus. Not unexpectedly, a primary difference between instillation and inflammation is that acute effects, such as acute inflammation, are higher in rats administered test substances by instillation compared to rats exposed to test substances by inhalation [80–83]. Another difference is that exposure by inhalation results in build up of the inspired material throughout the period of exposure. In contrast, administration by instillation results in the test material being deposited in the lung at the beginning of the study, allowing material-associated processes to proceed for the entire study period (Sect. 3.4 in [84]). In the case of MWCNT-7 induced mesothelioma, in the inhalation study conducted by the Japan Bioassay Research Center, at the end of the 2 year inhalation exposure to 2 mg/m<sup>3</sup> MWCNT-7 resulted in accumulation of 1.8 mg fibers in the lungs of male rats and 1468 fibers in the pleural area and mesothelial hyperplasia [17], while in the study by Numano et al. 2019 [20], instillation of 1.5 mg MWCNT-7 per rat, which is approximately the same level of MWCNT-7 that accumulated in the lungs of male rats exposed to 2 mg/m<sup>3</sup> MWCNT-7 by inhalation, the rats developed mesotheliomas. As argued by the authors, this suggests that if the study by JBRC could have been extended by an additional 12–18 months, inhalation exposure to MWCNT-7 would have resulted in the development of mesothelioma. However, most studies that compare the effects of administration by instillation and inhalation conclude that the toxicity of test substances administered by these two methods are similar. Two studies directly compared the pulmonary toxicity of MWCNTs administered by instillation and inhalation, and both studies found that both methods of administration resulted in similar pulmonary toxicities [85, 86]. Several other studies that administered nanoparticles using instillation and

inhalation also found both methods resulted in similar pulmonary toxicities [81, 82, 87–92]. Importantly, instillation of 2 mg potassium hexatitanate or 1 mg zinc oxide nanoparticles or 0.5 mg rutile type nano-TiO<sub>2</sub> per rat did not result in pulmonary toxicity [74, 93, 94], indicating that reasonable amounts of poorly soluble materials can be instilled into the rat lung without inducing particle overload associated pulmonary toxicity. Therefore, as stated by Oberdörster and Kuhlbusch, 2018, instillation studies are appropriate for hazard identification and hazard ranking, although instillation studies are not appropriate for hazard characterization [78].

## Conclusions

This is the first 2-year study to assess the toxicity and carcinogenicity of DWCNTs after administration into the rat lung. DWCNT did not induce toxic or carcinogenic effects in the pleural cavity, which is in agreement with long-term 2-year studies that found that rigid but not thin tangled CNTs induced mesothelioma when injected into the peritoneal cavity [18, 19, 21]. However, DWCNT administered at a dose of 0.5 mg/rat did cause pulmonary fibrosis and lung tumor development. This was most likely due to agglomerate formation by the fibers, resulting in biopersistence of the fibers in the lung and consequent chronic pulmonary inflammation which in turn promoted pulmonary fibrosis and tumor development. These results indicate that assessment of the toxicity of thin CNTs should not be based solely on the physicochemical characteristics of single fibers. In addition, the results of this study indicate that the possibility that DWCNTs may be toxic to humans cannot be ignored.

## Methods

### Nanomaterials

Two types of CNT were used in this study. DWCNT (brand name Tocana; Toray Industries, Inc., Tokyo, Japan) with an iron content below detectable limits and water content equal to 0.025% by weight (information provided by the company) and MWCNT-7 (Mitsui Chemicals Inc., Tokyo, Japan) with an iron content of 0.3% by weight [95]. Table 6 shows the water and iron content of the fibers.

### Animals

Nine-week old male F344 rats were purchased from Charles River Japan Inc. (Yukohama, Japan). The animals were housed in the Center for Experimental Animal Science of Nagoya City University Medical School, maintained on a 12 h light–dark cycle, and received Oriental MF basal diet (Oriental Yeast Co., Tokyo, Japan) and tap water ad libitum. The experimental protocol was approved by the Animal Care and Use Committee of Nagoya City University Medical School, and the research

**Table 6** Iron and water content of DWCNT and MWCNT-7 before dosing

	Iron content (wt%)	Water content (wt%)
DWCNT	0 <sup>a</sup>	0.025 <sup>a</sup>
MWCNT-7	0.3 <sup>b</sup>	NA <sup>c</sup>

<sup>a</sup> Information provided by Toray the manufacturer company

<sup>b</sup> Sakamoto et al. 2018[95]

<sup>c</sup> Not available

was conducted according to the Guidelines for the Care and Use of Laboratory Animals of Nagoya City University. The experiment was started after a 2-week acclimation and quarantine period.

### Experimental design

A total of 180 rats 11 weeks old were divided into six groups: Group 1 (26 rats) no treatment; Group 2 (30 rats) vehicle (saline with 0.5% Pluronic F-68; Sigma-Aldrich Merck); Group 3 (30 rats) DWCNT (0.125 mg/rat); Group 4 (33 rats) DWCNT (0.25 mg/rat); Group 5 (30 rats) DWCNT (0.5 mg/rat); and Group 6 (30 rats) MWCNT-7 (0.5 mg/rat): MWCNT-7 was used as the reference material. One rat in group 1 died before the 52 week interim sacrifice and was removed from the study, therefore, group 1 had 26 rats. Rats were administered the test solutions by TIPS as previously described [74]. Briefly, rats were anesthetized with 3% isoflurane and administered 0.5 ml vehicle or test material suspensions (15.6 µg, 31.25, or 62.5 µg of test material in 0.5 ml vehicle) using a micro sprayer (series IA–1B Intratracheal Aerosolizer Penn-century, Philadelphia, PA). Rats were administered one dose every other day over a 15-day period (8 administrations for total doses of 0.125, 0.25, or 0.5 mg DWCNT per rat and 0.5 mg MWCNT per rat). The amount of DWCNT administered to the rats was approximately equivalent to or less than the doses used in the studies by Crouzier et al., Tian et al., Sager et al., and El-Gazzar et al. [26–28, 30]. The dose of MWCNT-7 was one third the amount of MWCNT-7 that caused mesothelioma in rats in a previous study [20]. At week 52 an interim sacrifice was performed on 5 rats from the Untreated and Vehicle groups, 5 rats from the DWCNT 0.125 mg/rat group, 7 rats from the DWCNT 0.25 mg/rat group, 6 rats from the DWCNT-0.5 mg/rat group, and 5 rats from the MWCNT-7 group. All animals found moribund after 52 weeks underwent terminal sacrifice. Because of the loss of 16 animals by the end of week 90 in the MWCNT-7 group, final terminal sacrifice of the remaining 9 animals in this group was performed at week

91. Final terminal sacrifice of the untreated, vehicle, and DWCNT treated rats was at week 104. Final sacrifice refers to the terminal sacrifices performed at weeks 91 and 104.

#### Preparation of the test materials

Test materials were weighed and dispersed in tert-butyl alcohol by sonication for 10 min and stored frozen at  $-20^{\circ}\text{C}$ . Shortly before administration, the T-butyl alcohol was removed using an Eyela Freeze Drying machine (FDU-2110; Tokyo Rikakikai Co., Ltd., Tokyo, Japan), and the DWCNT and MWCNT-7 were suspended in saline containing 0.5% Pluronic F-68 (PF68, Sigma-Aldrich Merck) at 31.25, 62.5, and 125  $\mu\text{g}/\text{ml}$ . After suspension in Saline + PF68, test materials were sonicated for 2 min four times at 3000 rpm using a polytron PT 1600E bench top homogenizer (Kinematika AG, Lattau, Switzerland). Immediately prior to administration, the suspensions were sonicated for 30 min using a Tomy Ultrasonic disruptor, UD-211, equipped with a TP-040 micro tip (Tomy Seiko Co., Ltd., Tokyo, Japan) at a power setting of 4.

#### Characterization of the test materials before and after TIPS administration

After sonication, described above, and before administration to the rats' lungs, 20  $\mu\text{l}$  of each test material suspension was placed on a micro grid membrane pasting copper mesh (EMS 200-Cu, Nisshin EM Co., Ltd., Tokyo, Japan) for measurement of DWCNT and MWCNT-7 prior to TIPS administration. For measurement of DWCNT and MWCNT-7 in the lungs of rats at 52 and at the final sacrifice weeks after instillation about 1 gm of paraformaldehyde fixed lung tissue was digested as previously described [96]. Briefly, tissues were incubated in Clean 99-K200<sup>®</sup> (Clean chemical Co., Ltd., Ibraki, Japan) overnight or until complete dissolution of lung tissues. The digested solution was then centrifuged at 12,000 rpm for 30 min and the supernatant was discarded. The pellet was resuspended in distilled water and sonicated by a short burst (approximately 2–3 s) from a microson ultrasonic cell disruptor (Misonix Incorporated). The pellet was collected by centrifugation and washed two more times. After a final centrifugation, the pellet was resuspended in 200  $\mu\text{l}$  of distilled water and the specimens were collected on EMD Millipore<sup>TM</sup> Polycarbonate Membrane Filters (Millipore, Tokyo, Japan). Fibers were viewed by SEM (Field Emission Scanning Electronic Microscope; Hitachi High Technologies, Tokyo, Japan) at 5–10 kV and TEM (Transmission electron microscope; EDAX, Tokyo, Japan) at 15–50 K. Photos were analyzed by NIH image analyzer software (NIH, Bethesda, Maryland, USA). At least 200–300 fibers of each type of CNT were measured.

#### In vitro biodegradation

DWCNT and MWCNT-7 fibers were added to cultures of RAW cells, a mouse macrophage cell line, and to plates without cells (control). Cultures were incubated overnight with the CNTs at  $37^{\circ}\text{C}$  in a humidified incubator. The cells were washed twice with PBS to remove materials not associated with the cells. Control plates were not handled. The cultures were then incubated for an additional 4 days. After 5 days incubation with CNTs, culture media was removed from the RAW cell cultures, and the cells were washed twice with PBS to remove materials not associated with the cells. The cells were then harvested and the CNTs recovered from the cells. For the control plates, the CNTs were collected from the cell-free culture media. The collected CNTs were measured using far-infrared absorption to estimate the effective CNT length [97].

#### Electron microscopic viewing of fibers in lung tissues

For high magnification viewing, H&E stained slides were immersed in xylene to remove the cover glass, dried, and processed for SEM (Model S Field Emission SEM; Hitachi High Technologies, Tokyo, Japan). For ultrafine viewing, a small piece of paraformaldehyde fixed lung tissue was imbedded in epoxy resin and processed for TEM (EDAX, Tokyo, Japan).

#### Measurement of DWCNT and MWCNTs in the lung

Measurement of the amount of CNT fibers in the lung tissue was performed as described previously [23, 96].

#### Tissue sample collection and histopathological examination

At necropsy, blood samples were collected via the abdominal aorta under deep isoflurane anesthesia and serum samples were stored at  $-80^{\circ}\text{C}$ . Organs, including lung, liver, kidney, spleen, brain, heart, and testes were examined for any macroscopic lesions. The trachea, esophagus, lymph nodes (including mediastinal lymph nodes), diaphragm including the diaphragmatic region of the parietal pleura were examined macroscopically and then processed and examined histopathologically.

The 4 right lobes of the lung of each rat were excised at necropsy, frozen in liquid nitrogen, and stored at  $-80^{\circ}\text{C}$  for further biochemical analysis. The remaining left lung was inflated and fixed with 4% paraformaldehyde solution in phosphate-buffered saline (PBS) adjusted to pH 7.3 and processed for light microscopic examination. H&E stained tissue sections were evaluated by two board-certified Pathologists of the Japanese society of Toxicologic pathology, Drs. Hiroyuki Tsuda



and Satoru Takahashi, and diagnosis of hyperplasia, adenoma, adenocarcinoma, and mesothelioma was done according to the INHAND criteria [98].

PCNA staining of deparaffinized slides processed for antigen retrieval and blockade of endogenous peroxidase activity was performed as previously described [99]. For each lung specimen more than 1000 pulmonary epithelial cells and more than 500 visceral pleural and parietal pleural mesothelial cells were counted blindly in random fields. All nuclei showing brown staining of more than half of the nucleus were considered to be positive.

To determine the degree of inflammation the number of macrophages per  $\text{cm}^2$  of lung tissue was determined: Deparaffinized slides processed for antigen retrieval and blockade of endogenous peroxidase activity were incubated with PBS containing 5% BSA and 5% goat serum for 1 h, then incubated with the macrophage marker anti-CD68 (BMA Biomedicals, August, Switzerland) diluted 1:2000 in PBS containing 1% BSA and 1% goat serum overnight at 4 °C. After overnight incubation, the slides were incubated with secondary antibody (Nichirei Biosciences, Tokyo, Japan) for 1 h, visualized with DAB (Nichirei Biosciences, Tokyo, Japan), and counterstained with hematoxylin. Light microscopic images representing at least one  $\text{cm}^2$  from each lung were used to determine the density of the macrophages in the lungs.

Collagen deposition in lung tissues and visceral and partial pleura was quantified in light microscopic images of lung tissues and pleural sections stained with Masson's Trichrome (Abcam, Tokyo, Japan) using NIH image analyzer software (NIH, Bethesda, Maryland, USA): ten individual images were captured from 2 lung and 3 diaphragm sections from 3 rats per study group. Thresholding using pre-defined RGB criteria for collagen deposition was performed. This allowed collagen to be differentiated from alveolar tissue or pleural tissue. The surface area of fibrosed tissue was measured. Total lung alveolar and pleural tissue surface areas were measured individually by thresholding using predefined RGB criteria for lung alveolar and pleural tissues. The results are expressed as the percentage area of pulmonary collagen deposition per tissue surface area.

#### HMGB1 ELISA

At the final necropsy pleural lavage fluid collection was done for all rats as previously described [99]. High mobility group box protein 1 (HMGB1) was measured using a rat HMGB1 ELISA kit (Arigo Biolaboratories; ARG81310) according to the manufacturer's instructions.

#### CCL2 and CCL3 ELISA

Frozen right lung tissue samples (approximately 100 mg) were thawed and rinsed 3 times with ice-cold PBS and

homogenized in 1 mL tissue protein extraction reagent (Thermo Scientific, Rockford, IL, USA) containing 1% (v/v) protease inhibitor cocktail (Sigma-Aldrich Merck). The homogenates were centrifuged at 12000 g for 5 min at 4 °C. Protein content of the supernatant was measured using the BCA Protein Assay Kit (Pierce Biotech). The levels of CCL2 and CCL3 in the supernatant were measured using a Rat MCP-1/CCL2 ELISA Kit (Sigma-Aldrich Merck; RAB0058) and a CCL3 ELISA Kit (LSBio; LS-F5526) according to the manufacturers' instructions.

#### Detection of DNA adductomes in the lung tissue

Rat lung DNA was extracted by Genra<sup>®</sup> Puregene cell and tissue kit (Qiagen). The DNA (50  $\mu\text{g}$ ) was digested by incubation at 37 °C for 12 h in 300  $\mu\text{l}$  of 5 mM Tris-HCl (pH7.4) containing 50 units of DNaseI, 1 unit of Nuclease P1, 2 units of alkaline phosphatase, and 0.225 units of phosphodiesterase. After digestion, internal standards (100 pmol of 2',3'-dideoxyinosine and 2',3'-dideoxyadenosine) were added to the DNA hydrolysates. The hydrolysates were filtered through Amicon Ultra 3 kDa centrifugal filters (Sigma-Aldrich Merck; Z677094), and 500  $\mu\text{l}$  of methanol was added to the purified samples. After centrifugation and removal of the methanol, residual methanol was removed by evaporated *in vacuo*. DNA residues were dissolved in 100  $\mu\text{l}$  of 50% methanol, and 10  $\mu\text{l}$  of sample was subjected to LC/MS.

UHPLC-TOF-MS analyses was performed with a Shimadzu UHPLC Nexera X2 system (Shimadzu) using a Synergi Hydro-RP column (2.5  $\mu\text{m}$ , 100 mm  $\times$  2 mm, Phenomenex) and Triple TOF 5600+ (SCIEX) with an electrospray ionization device running in the positive ion mode. The detector conditions were as follows: ion spray voltage at 5500 V, source temperature of 350 °C, ion source gas 1, 60 psi, ion source gas 2 60 psi, declustering potential 80 V, collision energies of 45 V, and collision energy spread 15 V. Nitrogen was used as the collision gas. DNA adducts were detected using the MRM<sup>HR</sup> mode. This strategy was designed to detect the neutral loss of 2'-deoxyribose from positively ionized 2'-deoxynucleoside adducts by monitoring the samples with  $[M + H]^+ \rightarrow [M + H - 116]^+$  transitions [100]. In the mobile phases used for LC-TOF-MS analyses, solvent A consisted of a 0.1% (v/v) solution of formic acid in water and solvent B consisted of a 0.1% (v/v) solution of formic acid in acetonitrile. The DNA adducts were eluted from the column using a linear gradient, which started at 95% solvent A and 5% solvent B, and progressed to 100% solvent B over a period of 10 min. The system was then eluted with 100% solvent B for 10 min before being returned to the initial conditions over a period of 10 min to allow for the equilibration of the column. The system

was operated at a constant flow rate of 0.2 ml/min for all of the analyses.

### Statistical analysis

Survival rates were analyzed using the Kaplan–Meier method. The incidences of bronchioloalveolar hyperplasia, bronchioloalveolar adenoma, bronchioloalveolar carcinoma, and total lung tumor incidences were analyzed for difference from vehicle controls using GraphPad's Fisher's exact test (one-sided for comparison of treated rats to the vehicle controls and two-sided for comparison of DWCNT and MWCNT treated rats), and continuous data was analyzed using GraphPad's QuickCals t-Test Calculator. All data are expressed as mean  $\pm$  standard deviation. *p*-values  $< 0.05$  were considered to be significant.

### Supplementary Information

The online version contains supplementary material available at <https://doi.org/10.1186/s12989-022-00469-8>.

**Additional file 1: Figure S1.** Adductome maps of rats at 52 weeks. The relative peak areas and the number of peaks are given for each group. There were no significant differences in either peak area or the number of peaks between any of the groups. No adducts specific to any of the treated groups were found.

### Acknowledgements

The authors would like to acknowledge Toray Industries Inc. Tokyo Japan for provision of DWCNT and Drs. Takahiro Morimoto and Toshiya Okazaki, CNT-Application Research Center, National Institute of Advanced Industrial Science and Technology (AIST) for measurement of DWCNT and MWCNT-7.

### Authors' contributions

DMS and WA helped prepare and administer the materials used in the study, directed pathological examination, collected and prepared tissue samples, analyzed tissue samples, and drafted and wrote the manuscript. SL, JX, SS, and AN contributed to the conception and design of the study and assisted in pathological examination. OHMA, SG, H Takase, and MO characterized the materials used in this study and characterized lung inflammation. DA helped prepare and administer the materials used in the study and assisted in writing the manuscript. AE-G and MA helped prepare and administer the materials used in the study and assisted in animal care and well-being. TN directed administration of the materials used in the study, collected and prepared tissue samples, and was in charge of animal care and well-being. S Tomono and KF contributed to the conception and design of the study and analyzed DNA adducts. RHAH contributed to the conception and design of the study and assisted in writing the manuscript. JK, AH, MO, and S Takahashi contributed to the conception and design of the study, assisted in pathological analysis and analysis of tissue samples, and assisted in writing the manuscript. H Tsuda acquired funding for the study, and contributed to the conception and design of the study, assisted in writing the manuscript, and gave final approval of the manuscript submitted for publication. All authors read and approved the final manuscript.

### Funding

This study was supported by Research Grants from the Long-range Research Initiative, LRI, (2017–2019) of the Japan Chemical Industry Association; Health and Labour Sciences Research Grants from the Ministry of Health, Labour and Welfare, Japan (H27-kagaku-shitei-004, H30-kagaku-shitei-004, H25-kagaku-ippan-004, H28-kagaku-ippan-004); YOG Specified Nonprofit Corporation, Association for Promotion of Research on Risk Assessment (2018–2021); and

the Cultural Affairs and Missions Sector, Ministry of higher education of the Arab republic of Egypt.

### Availability of data and materials

All data generated or analysed during this study are included in this published article and its supplementary information files.

### Declarations

#### Ethics approval and consent to participate

Not applicable.

#### Consent for publication

Not applicable.

#### Competing interests

The authors declare that they have no competing interests.

#### Author details

<sup>1</sup>Nanotoxicology Lab Project, Nagoya City University, 3-1 Tanabe-Dohri, Mizuho-ku, Nagoya 467-8603, Japan. <sup>2</sup>Department of Experimental Pathology and Tumor Biology, Graduate School of Medical Sciences, Nagoya City University, Nagoya, Japan. <sup>3</sup>Department of Forensic Medicine and Clinical Toxicology, Faculty of Medicine, Assuit University, Assuit, Egypt. <sup>4</sup>College of Basic Medical Sciences, Anhui Medical University, Hefei, China. <sup>5</sup>Department of Forensic Medicine and Clinical Toxicology, Faculty of Medicine, Aswan University, Aswan, Egypt. <sup>6</sup>Department of Forensic Medicine and Toxicology, Faculty of Veterinary Medicine, Alexandria University, Alexandria, Egypt. <sup>7</sup>Department of Forensic Medicine and Toxicology, Faculty of Veterinary Medicine, Beni-Suef University, Beni-Suef, Egypt. <sup>8</sup>Department of Pediatrics and Human Development, Michigan State University, Michigan, USA. <sup>9</sup>Core Laboratory, Graduate School of Medicine, Nagoya City University, Nagoya, Japan. <sup>10</sup>Japan Industrial Safety and Health Association, Japan Bioassay Research Center, Hadano, Kanagawa, Japan. <sup>11</sup>Department of Microbiology and Immunology, Aichi Medical University School of Medicine, Nagakute, Japan. <sup>12</sup>Department of Neurotoxicology, Graduate School of Medical Sciences, Nagoya City University, Nagoya, Japan. <sup>13</sup>National Institute Hygienic Sciences, Kawasaki, Japan. <sup>14</sup>Department of Immunology, School of Basic Medical Sciences, Anhui Medical University, Hefei, China. <sup>15</sup>Department of Molecular Pathology, Osaka Metropolitan University Graduate School of Medicine, Osaka, Japan.

Received: 3 December 2021 Accepted: 7 April 2022

Published online: 22 April 2022

### References

- Ibrahim K. Carbon nanotubes-properties and applications: a review. *Carbon letters*. 2013;14:131–44. <https://doi.org/10.5714/CL.2013.14.3.131>.
- Bergamaschi E, Garzaro G, Wilson Jones G, Buglisi M, Caniglia M, Godono A, et al. Occupational exposure to carbon nanotubes and carbon nanofibres: more than a cobweb. *Nanomaterials* (Basel). 2021;11:3. <https://doi.org/10.3390/nano11030745>.
- Fadeel B, Kostarelos K. Grouping all carbon nanotubes into a single substance category is scientifically unjustified. *Nat Nanotechnol*. 2020;15(3):164. <https://doi.org/10.1038/s41565-020-0654-0>.
- Fischman M, Murashov V, Borak J, Seward J. Nanotechnology ATFo. *Health nanotechnology and Health*. *J Occup Environ Med*. 2019;61(3):e95–8. <https://doi.org/10.1097/JOM.0000000000001548>.
- Hansen SF, Lennquist A. Carbon nanotubes added to the SIN List as a nanomaterial of very high concern. *Nat Nanotechnol*. 2020;15(1):3–4. <https://doi.org/10.1038/s41565-019-0613-9>.
- Heller DA, Jena PV, Pasquali M, Kostarelos K, Delogu LG, Meidl RE, et al. Banning carbon nanotubes would be scientifically unjustified and damaging to innovation. *Nat Nanotechnol*. 2020;15(3):164–6. <https://doi.org/10.1038/s41565-020-0656-y>.
- Schulte PA, Leso V, Niang M, Iavicoli I. Current state of knowledge on the health effects of engineered nanomaterials in workers: a systematic review of human studies and epidemiological investigations. *Scand J*

- Work Environ Health. 2019;45(3):217–38. <https://doi.org/10.5271/sjweh.3800>.
8. Hansen SF, Lennquist A. SIN List criticism based on misunderstandings. *Nat Nanotechnol*. 2020;15(6):418. <https://doi.org/10.1038/s41565-020-0692-7>.
  9. Coussens LM, Werb Z. Inflammation and cancer. *Nature*. 2002;420(6917):860–7. <https://doi.org/10.1038/nature01322>.
  10. IARC. Arsenic, metals, fibres, and dusts. Volume 100C. 2012. <http://monographs.iarc.fr/ENG/Monographs/vol100C/mono100C.pdf>. Accessed 26 Jan 2022.
  11. IARC. Some nanomaterials and some fibres. Volume 111. 2017. <http://monographs.iarc.fr/ENG/Monographs/vol111/mono111.pdf>. Accessed 26 Jan 2022.
  12. Okada F, Fujii J. Molecular mechanisms of inflammation-induced carcinogenesis. *J Clin Biochem Nutr*. 2006;39(3):103–13. <https://doi.org/10.3164/jcbn.39.103>.
  13. Pollard KM. Silica, silicosis, and autoimmunity. *Front Immunol*. 2016;7:97. <https://doi.org/10.3389/fimmu.2016.00097>.
  14. Topinka J, Loli P, Georgiadis P, Dusinska M, Hurbankova M, Kovacikova Z, et al. Mutagenesis by asbestos in the lung of lambda-Ia-cl transgenic rats. *Mutat Res*. 2004;553(1–2):67–78. <https://doi.org/10.1016/j.mrfmmm.2004.06.023>.
  15. Yang H, Testa JR, Carbone M. Mesothelioma epidemiology, carcinogenesis, and pathogenesis. *Curr Treat Options Oncol*. 2008;9(2–3):147–57. <https://doi.org/10.1007/s11864-008-0067-z>.
  16. Honda K, Naya M, Takehara H, Kataura H, Fujita K, Ema M. A 104-week pulmonary toxicity assessment of long and short single-wall carbon nanotubes after a single intratracheal instillation in rats. *Inhal Toxicol*. 2017;29(11):471–82. <https://doi.org/10.1080/08958378.2017.1394930>.
  17. Kasai T, Umeda Y, Ohnishi M, Mine T, Kondo H, Takeuchi T, et al. Lung carcinogenicity of inhaled multi-walled carbon nanotube in rats. *Part Fibre Toxicol*. 2016;13(1):53. <https://doi.org/10.1186/s12989-016-0164-2>.
  18. Muller J, Delos M, Panin N, Rabolli V, Huaux F, Lison D. Absence of carcinogenic response to multiwall carbon nanotubes in a 2-year bioassay in the peritoneal cavity of the rat. *Toxicol Sci*. 2009;110(2):442–8. <https://doi.org/10.1093/toxsci/kfp100>.
  19. Nagai H, Okazaki Y, Chew SH, Misawa N, Miyata Y, Shinohara H, et al. Intraperitoneal administration of tangled multiwalled carbon nanotubes of 15 nm in diameter does not induce mesothelial carcinogenesis in rats. *Pathol Int*. 2013;63(9):457–62. <https://doi.org/10.1111/pin.12093>.
  20. Numano T, Higuchi H, Alexander DB, Alexander WT, Abdelgied M, El-Gazzar AM, et al. MWCNT-7 administered to the lung by intratracheal instillation induces development of pleural mesothelioma in F344 rats. *Cancer Sci*. 2019;110(8):2485–92. <https://doi.org/10.1111/cas.14121>.
  21. Rittinghausen S, Hackbarth A, Creutzenberg O, Ernst H, Heinrich U, Leonhardt A, et al. The carcinogenic effect of various multi-walled carbon nanotubes (MWCNTs) after intraperitoneal injection in rats. *Part Fibre Toxicol*. 2014;11:59.
  22. Saleh DM, Alexander WT, Numano T, Ahmed OHM, Gunasekaran S, Alexander DB, et al. Comparative carcinogenicity study of a thick, straight-type and a thin, tangled-type multi-walled carbon nanotube administered by intra-tracheal instillation in the rat. *Part Fibre Toxicol*. 2020;17(1):48. <https://doi.org/10.1186/s12989-020-00382-y>.
  23. Suzui M, Futakuchi M, Fukamachi K, Numano T, Abdelgied M, Takahashi S, et al. Multiwalled carbon nanotubes intratracheally instilled into the rat lung induce development of pleural malignant mesothelioma and lung tumors. *Cancer Sci*. 2016;107(7):924–35. <https://doi.org/10.1111/cas.12954>.
  24. Fujita K, Fukuda M, Fukui H, Horie M, Endoh S, Uchida K, et al. Intratracheal instillation of single-wall carbon nanotubes in the rat lung induces time-dependent changes in gene expression. *Nanotoxicology*. 2015;9(3):290–301. <https://doi.org/10.3109/17435390.2014.921737>.
  25. Tsuda H, Alexander DB. Development of Intratracheal Intrapulmonary Spraying (TIPS) administration as a feasible assay method for testing the toxicity and carcinogenic potential of multiwall carbon nanotubes. In vivo inhalation toxicity screening methods for manufactured nanomaterials. Berlin: Springer; 2019. p. 145–63.
  26. Crouzier D, Follot S, Gentilhomme E, Flahaut E, Arnaud R, Dabouis V, et al. Carbon nanotubes induce inflammation but decrease the production of reactive oxygen species in lung. *Toxicology*. 2010;272(1–3):39–45. <https://doi.org/10.1016/j.tox.2010.04.001>.
  27. Tian F, Habel NC, Yin R, Hirn S, Banerjee A, Ercal N, et al. Pulmonary DWCNT exposure causes sustained local and low-level systemic inflammatory changes in mice. *Eur J Pharm Biopharm*. 2013;84(2):412–20. <https://doi.org/10.1016/j.ejpb.2013.03.008>.
  28. Sager TM, Wolfarth MW, Battelli LA, Leonard SS, Andrew M, Steinbach T, et al. Investigation of the pulmonary bioactivity of double-walled carbon nanotubes. *J Toxicol Environ Health A*. 2013;76(15):922–36. <https://doi.org/10.1080/15287394.2013.825571>.
  29. O'Shaughnessy PT, Adamcakova-Dodd A, Altmaier R, Thorne PS. Assessment of the aerosol generation and toxicity of carbon nanotubes. *Nanomaterials (Basel)*. 2014;4(2):439–53. <https://doi.org/10.3390/nano4020439>.
  30. El-Gazzar AM, Abdelgied M, Alexander DB, Alexander WT, Numano T, Iigo M, et al. Comparative pulmonary toxicity of a DWCNT and MWCNT-7 in rats. *Arch Toxicol*. 2019;93(1):49–59. <https://doi.org/10.1007/s00204-018-2336-3>.
  31. Blackshear PE, Pandiri AR, Ton TV, Clayton NP, Shockley KR, Peddada SD, et al. Spontaneous mesotheliomas in F344/N rats are characterized by dysregulation of cellular growth and immune function pathways. *Toxicol Pathol*. 2014;42(5):863–76. <https://doi.org/10.1177/0192623313501894>.
  32. Napolitano A, Antoine DJ, Pellegrini L, Baumann F, Pagano I, Pastorino S, et al. HMGB1 and its hyperacetylated isoform are sensitive and specific serum biomarkers to detect asbestos exposure and to identify mesothelioma patients. *Clin Cancer Res*. 2016;22(12):3087–96. <https://doi.org/10.1158/1078-0432.CCR-15-1130>.
  33. Tabata C, Shibata E, Tabata R, Kanemura S, Mikami K, Nogi Y, et al. Serum HMGB1 as a prognostic marker for malignant pleural mesothelioma. *BMC Cancer*. 2013;13:205. <https://doi.org/10.1186/1471-2407-13-205>.
  34. Wang Y, Jiang Z, Yan J, Ying S. HMGB1 as a potential biomarker and therapeutic target for malignant mesothelioma. *Dis Markers*. 2019;2019:4183157. <https://doi.org/10.1155/2019/4183157>.
  35. Ying S, Jiang Z, He X, Yu M, Chen R, Chen J, et al. Serum HMGB1 as a potential biomarker for patients with asbestos-related diseases. *Dis Markers*. 2017;2017:5756102. <https://doi.org/10.1155/2017/5756102>.
  36. Yang H, Rivera Z, Jube S, Nasu M, Bertino P, Goparaju C, et al. Programmed necrosis induced by asbestos in human mesothelial cells causes high-mobility group box 1 protein release and resultant inflammation. *Proc Natl Acad Sci U S A*. 2010;107(28):12611–6. <https://doi.org/10.1073/pnas.1006542107>.
  37. Jube S, Rivera ZS, Bianchi ME, Powers A, Wang E, Pagano I, et al. Cancer cell secretion of the DAMP protein HMGB1 supports progression in malignant mesothelioma. *Cancer Res*. 2012;72(13):3290–301. <https://doi.org/10.1158/0008-5472.CAN-11-3481>.
  38. Qi F, Okimoto G, Jube S, Napolitano A, Pass HI, Laczko R, et al. Continuous exposure to chrysotile asbestos can cause transformation of human mesothelial cells via HMGB1 and TNF-alpha signaling. *Am J Pathol*. 2013;183(5):1654–66. <https://doi.org/10.1016/j.ajpath.2013.07.029>.
  39. Xue J, Patergnani S, Giorgi C, Suarez J, Goto K, Bononi A, et al. Asbestos induces mesothelial cell transformation via HMGB1-driven autophagy. *Proc Natl Acad Sci USA*. 2020;117(41):25543–52. <https://doi.org/10.1073/pnas.2007622117>.
  40. Tokarz DA, Gruebbel MM, Willson GA, Hardisty JF, Pearse G, Cesta MF. Spontaneous primary pleural mesothelioma in Fischer 344 (F344) and other rat strains: a retrospective review. *Toxicol Pathol*. 2021. <https://doi.org/10.1177/01926233211053631>.
  41. Chew SH, Toyokuni S. Malignant mesothelioma as an oxidative stress-induced cancer: an update. *Free Radic Biol Med*. 2015;86:166–78. <https://doi.org/10.1016/j.freeradbiomed.2015.05.002>.
  42. Donaldson K, Murphy FA, Duffin R, Poland CA. Asbestos, carbon nanotubes and the pleural mesothelium: a review of the hypothesis regarding the role of long fibre retention in the parietal pleura, inflammation and mesothelioma. *Part Fibre Toxicol*. 2010;7:5. <https://doi.org/10.1186/1743-8977-7-5>.
  43. Donaldson K, Poland CA, Murphy FA, MacFarlane M, Chernova T, Schinwald A. Pulmonary toxicity of carbon nanotubes and

- asbestos—similarities and differences. *Adv Drug Deliv Rev.* 2013;65(15):2078–86. <https://doi.org/10.1016/j.addr.2013.07.014>.
44. Miserocchi G, Sancini G, Mantegazza F, Chiappino G. Translocation pathways for inhaled asbestos fibers. *Environ Health.* 2008;7:4. <https://doi.org/10.1186/1476-069X-7-4>.
  45. Roe OD, Stella GM. Malignant pleural mesothelioma: history, controversy and future of a manmade epidemic. *Eur Respir Rev.* 2015;24(135):115–31. <https://doi.org/10.1183/09059180.00007014>.
  46. Stellaa GM. Carbon nanotubes and pleural damage: perspectives of nanosafety in the light of asbestos experience. *Biointerphases.* 2011;6(2):P1–17. <https://doi.org/10.1116/1.3582324>.
  47. Walter D. Primary particles—agglomerates—aggregates. *Nanomaterials.* 2013;9–24.
  48. Johnston HJ, Hutchison GR, Christensen FM, Peters S, Hankin S, Aschberger K, et al. A critical review of the biological mechanisms underlying the in vivo and in vitro toxicity of carbon nanotubes: the contribution of physico-chemical characteristics. *Nanotoxicology.* 2010;4(2):207–46. <https://doi.org/10.3109/17435390903569639>.
  49. Laux P, Riebeling C, Booth AM, Brain JD, Brunner J, Cerrillo C, et al. Biokinetics of nanomaterials: the role of biopersistence. *NanolImpact.* 2017;6:69–80. <https://doi.org/10.1016/j.impact.2017.03.003>.
  50. Dahm MM, Schubauer-Berigan MK, Evans DE, Birch ME, Fernback JE, Deddens JA. Carbon nanotube and nanofiber exposure assessments: an analysis of 14 site visits. *Ann Occup Hyg.* 2015;59(6):705–23. <https://doi.org/10.1093/annhyg/mev020>.
  51. Dong J. Microenvironmental alterations in carbon nanotube-induced lung inflammation and fibrosis. *Front Cell Dev Biol.* 2020;8:126. <https://doi.org/10.3389/fcell.2020.00126>.
  52. Dong J, Ma Q. Integration of inflammation, fibrosis, and cancer induced by carbon nanotubes. *Nanotoxicology.* 2019;13(9):1244–74. <https://doi.org/10.1080/17435390.2019.1651920>.
  53. Ito T, Connett JM, Kunkel SL, Matsukawa A. The linkage of innate and adaptive immune response during granulomatous development. *Front Immunol.* 2013;4:10. <https://doi.org/10.3389/fimmu.2013.00010>.
  54. Petersen HJ, Smith AM. The role of the innate immune system in granulomatous disorders. *Front Immunol.* 2013;4:120. <https://doi.org/10.3389/fimmu.2013.00120>.
  55. Barbarino M, Giordano A. Assessment of the carcinogenicity of carbon nanotubes in the respiratory system. *Cancers (Basel).* 2021. <https://doi.org/10.3390/cancers13061318>.
  56. Cavallo F, De Giovanni C, Nanni P, Forni G, Lollini PL. 2011: the immune hallmarks of cancer. *Cancer Immunol Immunother.* 2011;60(3):319–26. <https://doi.org/10.1007/s00262-010-0968-0>.
  57. Colotta F, Allavena P, Sica A, Garlanda C, Mantovani A. Cancer-related inflammation, the seventh hallmark of cancer: links to genetic instability. *Carcinogenesis.* 2009;30(7):1073–81. <https://doi.org/10.1093/carcin/bgp127>.
  58. Hanahan D, Weinberg RA. Hallmarks of cancer: the next generation. *Cell.* 2011;144(5):646–74. <https://doi.org/10.1016/j.cell.2011.02.013>.
  59. Dong J, Ma Q. Type 2 immune mechanisms in carbon nanotube-induced lung fibrosis. *Front Immunol.* 2018;9:1120. <https://doi.org/10.3389/fimmu.2018.01120>.
  60. Dong J, Ma Q. In vivo activation and pro-fibrotic function of NF-kappaB in fibroblastic cells during pulmonary inflammation and fibrosis induced by carbon nanotubes. *Front Pharmacol.* 2019;10:1140. <https://doi.org/10.3389/fphar.2019.01140>.
  61. Wynn TA. Cellular and molecular mechanisms of fibrosis. *J Pathol.* 2008;214(2):199–210. <https://doi.org/10.1002/path.2277>.
  62. Sayan M, Mossman BT. The NLRP3 inflammasome in pathogenic particle and fibre-associated lung inflammation and diseases. *Part Fibre Toxicol.* 2016;13(1):51. <https://doi.org/10.1186/s12989-016-0162-4>.
  63. Kane AB, Organization WH. Mechanisms of fibre carcinogenesis. 2000. IARC Scientific Publications No. 140 <https://publications.iarc.fr/Book-And-Report-Series/Iarc-Scientific-Publications/Mechanisms-Of-Fibre-Carcinogenesis-1996>
  64. Nagai H, Okazaki Y, Chew SH, Misawa N, Yamashita Y, Akatsuka S, et al. Diameter and rigidity of multiwalled carbon nanotubes are critical factors in mesothelial injury and carcinogenesis. *Proc Natl Acad Sci U S A.* 2011;108(49):E1330–8. <https://doi.org/10.1073/pnas.1110013108>.
  65. Canu IG, Batsungnoen K, Maynard A, Hopf N. State of knowledge on the occupational exposure to carbon nanotubes. *Int J Hyg Environ Health.* 2020;225: 113472. <https://doi.org/10.1016/j.ijheh.2020.113472>.
  66. Dahm MM, Evans DE, Schubauer-Berigan MK, Birch ME, Deddens JA. Occupational exposure assessment in carbon nanotube and nanofiber primary and secondary manufacturers: mobile direct-reading sampling. *Ann Occup Hyg.* 2013;57(3):328–44. <https://doi.org/10.1093/annhyg/mes079>.
  67. Kuijpers E, Pronk A, Kleemann R, Vlaanderen J, Lan Q, Rothman N, et al. Cardiovascular effects among workers exposed to multiwalled carbon nanotubes. *Occup Environ Med.* 2018;75(5):351–8. <https://doi.org/10.1136/oemed-2017-104796>.
  68. Schubauer-Berigan MK, Dahm MM, Erdely A, Beard JD, Eileen Birch M, Evans DE, et al. Association of pulmonary, cardiovascular, and hematologic metrics with carbon nanotube and nanofiber exposure among US workers: a cross-sectional study. *Part Fibre Toxicol.* 2018;15(1):22. <https://doi.org/10.1186/s12989-018-0258-0>.
  69. Stone KC, Mercer RR, Gehr P, Stockstill B, Crapo JD. Allometric relationships of cell numbers and size in the mammalian lung. *Am J Respir Cell Mol Biol.* 1992;6(2):235–43. <https://doi.org/10.1165/ajrcmb.6.2.235>.
  70. US EPA. Air Quality Criteria for Particulate Matter. 2004. <http://cites.eerx.ist.psu.edu/viewdoc/download?doi=10.1.1.400.5005&rep=rep1&type=pdf> Accessed 26 Jan 2022.
  71. Rodelsperger K, Woitowitz HJ. Airborne fibre concentrations and lung burden compared to the tumour response in rats and humans exposed to asbestos. *Ann Occup Hyg.* 1995;39(5):715–25.
  72. Bignon J, Brochard P, Brown R, Davis J, Vu V, Gibbs G, et al. Assessment of the toxicity of man-made fibres: a final report of a workshop held in Paris, France 3–4 February 1994. *Ann Occup Hyg.* 1995;39(1):89–106. [https://doi.org/10.1016/0003-4878\(94\)00126-L](https://doi.org/10.1016/0003-4878(94)00126-L).
  73. Zumwalde RD. Occupational exposure to carbon nanotubes and nanofibers. 2013. <https://stacks.cdc.gov/view/cdc/13522> Accessed 26 Jan 2022.
  74. Abdelgied M, El-Gazzar AM, Alexander WT, Numano T, Iigou M, Naiki-Ito A, et al. Carcinogenic effect of potassium octatitanate (POT) fibers in the lung and pleura of male Fischer 344 rats after intrapulmonary administration. *Part Fibre Toxicol.* 2019;16(1):34. <https://doi.org/10.1186/s12989-019-0316-2>.
  75. Bevan RJ, Kreiling R, Levy LS, Warheit DB. Toxicity testing of poorly soluble particles, lung overload and lung cancer. *Regul Toxicol Pharmacol.* 2018;100:80–91. <https://doi.org/10.1016/j.yrtph.2018.10.006>.
  76. Driscoll KE, Borm PJA. Expert workshop on the hazards and risks of poorly soluble low toxicity particles. *Inhal Toxicol.* 2020;32(2):53–62. <https://doi.org/10.1080/08958378.2020.1735581>.
  77. IARC monographs on the identification of carcinogenic hazards to humans. PREAMBLE (amended January 2019). <https://monographs.iarc.who.int/wp-content/uploads/2019/07/Preamble-2019.pdf> Accessed 25 Jan 2022.
  78. Oberdörster G, Kuhlbusch TA. In vivo effects: methodologies and biokinetics of inhaled nanomaterials. *NanolImpact.* 2018;10:38–60. <https://doi.org/10.1016/j.impact.2017.10.007>.
  79. Bos PMJ, Gogens I, Geraets L, Delmaar C, Cassee FR. Pulmonary toxicity in rats following inhalation exposure to poorly soluble particles: The issue of impaired clearance and the relevance for human health hazard and risk assessment. *Regul Toxicol Pharmacol.* 2019;109:104498. <https://doi.org/10.1016/j.yrtph.2019.104498>.
  80. Baisch BL, Corson NM, Wade-Mercer P, Gelein R, Kennell AJ, Oberdorster G, et al. Equivalent titanium dioxide nanoparticle deposition by intratracheal instillation and whole body inhalation: the effect of dose rate on acute respiratory tract inflammation. *Part Fibre Toxicol.* 2014;11:5. <https://doi.org/10.1186/1743-8977-11-5>.
  81. Horie M, Yoshiura Y, Izumi H, Oyabu T, Tomonaga T, Okada T, et al. Comparison of the pulmonary oxidative stress caused by intratracheal instillation and inhalation of NiO nanoparticles when equivalent amounts of NiO are retained in the lung. *Antioxidants (Basel).* 2016. <https://doi.org/10.3390/antiox5010004>.
  82. Morimoto Y, Izumi H, Yoshiura Y, Tomonaga T, Oyabu T, Myojo T, et al. Pulmonary toxicity of well-dispersed cerium oxide nanoparticles following intratracheal instillation and inhalation. *J Nanopart Res.* 2015;17(11):442. <https://doi.org/10.1007/s11051-015-3249-1>.

83. Silva RM, Doudrick K, Franzi LM, TeeSy C, Anderson DS, Wu Z, et al. Instillation versus inhalation of multiwalled carbon nanotubes: exposure-related health effects, clearance, and the role of particle characteristics. *ACS Nano*. 2014;8(9):8911–31. <https://doi.org/10.1021/nn503887r>.
84. Fukushima S, Kasai T, Umeda Y, Ohnishi M, Sasaki T, Matsumoto M. Carcinogenicity of multi-walled carbon nanotubes: challenging issue on hazard assessment. *J Occup Health*. 2018;60(1):10–30.
85. Morimoto Y, Hirohashi M, Ogami A, Oyabu T, Myojo T, Todoroki M, et al. Pulmonary toxicity of well-dispersed multi-wall carbon nanotubes following inhalation and intratracheal instillation. *Nanotoxicology*. 2012;6(6):587–99. <https://doi.org/10.3109/17435390.2011.594912>.
86. Gate L, Knudsen KB, Seidel C, Berthing T, Chezeau L, Jacobsen NR, et al. *Toxicol Appl Pharmacol*. 2019;375:17–31. <https://doi.org/10.1016/j.taap.2019.05.001>.
87. Iwai K, Higuchi K, Udagawa T, Ohtomo K, Kawabata Y. Lung tumor induced by long-term inhalation or intratracheal instillation of diesel exhaust particles. *Exp Toxicol Pathol*. 1997;49(5):393–401. [https://doi.org/10.1016/S0940-2993\(97\)80125-X](https://doi.org/10.1016/S0940-2993(97)80125-X).
88. Li YS, Ootsuyama Y, Kawasaki Y, Morimoto Y, Higashi T, Kawai K. Oxidative DNA damage in the rat lung induced by intratracheal instillation and inhalation of nanoparticles. *J Clin Biochem Nutr*. 2018;62(3):238–41. <https://doi.org/10.3164/jcbn.17-70>.
89. Morimoto Y, Izumi H, Yoshiura Y, Tomonaga T, Lee BW, Okada T, et al. Comparison of pulmonary inflammatory responses following intratracheal instillation and inhalation of nanoparticles. *Nanotoxicology*. 2016;10(5):607–18. <https://doi.org/10.3109/17435390.2015.1104740>.
90. Oyabu T, Morimoto Y, Lee B-W, Okada T, Izumi H, Tomonaga T, et al. Biopersistence of nanoparticle in inhalation and intratracheal instillation studies for hazard assessment. *Eur Respir J*. 2014;44(Suppl):58.
91. Oyabu T, Myojo T, Lee BW, Okada T, Izumi H, Yoshiura Y, et al. Biopersistence of NiO and TiO<sub>2</sub> nanoparticles following intratracheal instillation and inhalation. *Int J Mol Sci*. 2017. <https://doi.org/10.3390/ijms18122757>.
92. Warheit DB, Brock WJ, Lee KP, Webb TR, Reed KL. Comparative pulmonary toxicity inhalation and instillation studies with different TiO<sub>2</sub> particle formulations: impact of surface treatments on particle toxicity. *Toxicol Sci*. 2005;88(2):514–24. <https://doi.org/10.1093/toxsci/kfi331>.
93. Morimoto Y, Izumi H, Yoshiura Y, Tomonaga T, Oyabu T, Myojo T, et al. Evaluation of pulmonary toxicity of zinc oxide nanoparticles following inhalation and intratracheal instillation. *Int J Mol Sci*. 2016. <https://doi.org/10.3390/ijms17081241>.
94. Yamamoto M, Oyabu T, Morimoto Y, Ogami A, Kadoya C, Nishi K, et al. Biopersistence of potassium hexatitanate in inhalation and intratracheal instillation studies. *Inhal Toxicol*. 2011;23(4):196–204. <https://doi.org/10.3109/08958378.2011.558935>.
95. Sakamoto Y, Hojo M, Kosugi Y, Watanabe K, Hirose A, Inomata A, et al. Comparative study for carcinogenicity of 7 different multi-wall carbon nanotubes with different physicochemical characteristics by a single intraperitoneal injection in male Fischer 344 rats. *J Toxicol Sci*. 2018;43(10):587–600. <https://doi.org/10.2131/jts.43.587>.
96. Ohnishi M, Yajima H, Kasai T, Umeda Y, Yamamoto M, Yamamoto S, et al. Novel method using hybrid markers: development of an approach for pulmonary measurement of multi-walled carbon nanotubes. *J Occup Med Toxicol*. 2013;8(1):30. <https://doi.org/10.1186/1745-6673-8-30>.
97. Morimoto T, Joung SK, Saito T, Futaba DN, Hata K, Okazaki T. Length-dependent plasmon resonance in single-walled carbon nanotubes. *ACS Nano*. 2014;8(10):9897–904. <https://doi.org/10.1021/nn505430s>.
98. Renne R, Brix A, Harkema J, Herbert R, Kittel B, Lewis D, et al. Proliferative and nonproliferative lesions of the rat and mouse respiratory tract. *Toxicol Pathol*. 2009;37(7 Suppl):5s–73s. <https://doi.org/10.1177/0192623309353423>.
99. Abdelgied M, El-Gazzar AM, Alexander DB, Alexander WT, Numano T, Iigou M, et al. Potassium octatitanate fibers induce persistent lung and pleural injury and are possibly carcinogenic in male Fischer 344 rats. *Cancer Sci*. 2018;109(7):2164–77. <https://doi.org/10.1111/cas.13643>.
100. Kanaly RA, Matsui S, Hanaoka T, Matsuda T. Application of the adductome approach to assess intertissue DNA damage variations in human lung and esophagus. *Mutat Res*. 2007;625(1–2):83–93. <https://doi.org/10.1016/j.mrfmmm.2007.05.006>.

## Publisher's Note

Springer Nature remains neutral with regard to jurisdictional claims in published maps and institutional affiliations.

Ready to submit your research? Choose BMC and benefit from:

- fast, convenient online submission
- thorough peer review by experienced researchers in your field
- rapid publication on acceptance
- support for research data, including large and complex data types
- gold Open Access which fosters wider collaboration and increased citations
- maximum visibility for your research: over 100M website views per year

At BMC, research is always in progress.

Learn more [biomedcentral.com/submissions](https://biomedcentral.com/submissions)

